Stochastic Model of Neuronal Outgrowth Movement: UNC-5 (UNC5) Regulates the Length and Number of Neuronal Processes in *Caenorhabditis elegans*

Gerard Limerick[*,†], Xia Tang[*,†], Won Suk Lee[*,†], Ahmed Mohamed[*], Aseel Al-Aamiri[*], and William G. Wadsworth[*]

[*]Department of Pathology and Laboratory Medicine, Rutgers Robert Wood Johnson Medical School, Piscataway, NJ 08854

†These authors contributed equally to this work

11 running title: neuronal outgrowth patterning

12

13 key words: neuronal development, axon guidance, asymmetric localization, *Caenorhabditis*

14 *elegans*, netrin and wnt signaling

15

16 corresponding author:

17 William G. Wadsworth

18 Department of Pathology and Laboratory Medicine

19 Rutgers Robert Wood Johnson Medical School

20 675 Hoes Lane West

21 Piscataway, NJ 08854-5635

22 732-235-5768

23 william.wadsworth@rwjms.rutgers.edu

Abstract

Neurons extend processes that vary in number, length, and direction of outgrowth. Extracellular cues help determine the patterning of outgrowth. In *Caenorhabditis elegans,* neurons respond to the extracellular UNC-6 (netrin) cue via UNC-40 (DCC) and UNC-5 (UNC5) receptors. We have postulated that UNC-40 undergoes stochastically orientated asymmetric localization (SOAL) within neurons. Extracellular cues govern the probability of UNC-40 localizing and mediating outgrowth at points along the surface of the neuron. For each instance of time there is a probability that UNC-40-mediated outgrowth will occur in a specific direction and so over time the direction of outgrowth fluctuates. Random walk modeling predicts that the degree of fluctuation affects the extent of outgrowth movement. Therefore, different patterns of outgrowth could be caused by regulating UNC-40 SOAL. Here we present evidence that UNC-5 (UNC5) receptor activity regulates UNC-40 SOAL and affects the length and number of processes that neurons develop. We find that loss of UNC-5 function increases the probability of UNC-40-mediated outgrowth in different directions, thereby increasing the degree of fluctuation. Consistent with the model, in *unc-5* loss-of-function mutants neurons fail to extend processes to full length or fail to develop multiple processes. We further show genetic interactions that suggest the UNC-5 and SAX-3 (Robo) receptors, and the cytoplasmic proteins, UNC-53 (NAV2), MIG-15 (NIK kinase), and MADD-2 (TRIM), function through specific signaling pathways to regulate UNC-40 SOAL in response to the UNC-6 and EGL-20 (wnt) extracellular cues. We propose genes influence the patterning of neuronal outgrowth by regulating the SOAL process.

Introduction

During development, an intricate network of neuronal connections is established. As processes extend from the neuronal cell bodies, distinct patterns of outgrowth emerge. Some extensions remain as a single process, whereas others branch and form multiple processes. If they branch, the extensions can travel in the same or in different directions. Processes vary in length. Extracellular cues are known to influence this patterning, but the underlying logic that governs the formation of patterns remains a mystery.

The secreted extracellular UNC-6 (netrin) molecule and its receptors, UNC-5 (UNC5) and UNC-40 (DCC) are highly conserved in invertebrates and vertebrates, and are known to play key roles in cell and axon migrations. In *Caenorhabditis elegans*, UNC-6 is produced by ventral cells in the midbody and by glia cells at the nerve ring in the head (WADSWORTH *et al.* 1996; WADSWORTH AND HEDGECOCK 1996; ASAKURA *et al.* 2007). It's been observed that neurons that express the receptor UNC-40 (DCC) extend axons ventrally, towards the UNC-6 sources; whereas neurons that express the receptor UNC-5 (UNC5) alone or in combination with UNC-40 extend axons dorsally, away from the UNC-6 sources (HEDGECOCK *et al.* 1990; LEUNG-HAGESTEIJN *et al.* 1992; CHAN *et al.* 1996; WADSWORTH *et al.* 1996).

It is commonly proposed that axons are guided by attractive and repulsive mechanisms (Tessier-Lavigne and Goodman 1996). According to this model, extracellular cues act as attractants or repellants to direct neuronal outgrowth towards or away from sources of the cues. UNC-5 (UNC5) has been described as a "repulsive" netrin receptor because it mediates guidance away from netrin sources (Leung-Hagesteijn et al. 1992; Hong et al. 1999; Keleman and Dickson 2001; Moore et al. 2007). The attraction and repulsion model is deterministic. That is, given the same

conditions, the response of the neuron, attractive or repulsive, will always be the same. As such, the neuronal response to a particular cue is thought to be mediated by attractive or repulsive signaling pathways. In genetic studies, a mutation that disrupts movement towards the cue source denotes gene function within an attractive pathway, whereas mutations that disrupt movement away from a source denotes gene function within a repulsive pathway. Furthermore, the model predicts that the responsiveness of a neuron must switch from attractive to repulsive if the axonal growth cone move towards and then away from the source of a cue.

We have proposed an alternative model in which the movement of neuronal outgrowth is established through a stochastic process. This model is based on evidence indicating that the asymmetrical localization of UNC-40 in the neuron is self-organizing and that the surface to which UNC-40 localizes and mediates outgrowth is stochastically determined (Figure 1A) (Xu *et al.* 2009; Kulkarni *et al.* 2013). Because of this process, which we name "stochastically orientated asymmetric localization" (SOAL), there is a probability that UNC-40-mediated outgrowth will take place at each point along the surface of the neuron. At any instance of time, extracellular cues govern the probability of UNC-40-mediated outgrowth at each point (Kulkarni *et al.* 2013; Tang and Wadsworth 2014; Yang *et al.* 2014). Outgrowth extension can be envisioned as a series of steps, where at each step extracellular cues control the probability for outgrowth in each direction from the point on the surface. This means that over time, the direction of outgrowth movement fluctuates. Such movement can be mathematically described as a random walk, *i.e.* a succession of randomly directed steps (Figure 1B). Random walk movement is diffusive and one property of diffusive motion is that the mean square displacement grows proportionate to the time traveled. Consequently, the more the direction of movement fluctuates, the shorter the distance of travel is in a given amount of time (Figure

1B). In this paper, we propose that UNC-5 helps regulate this fluctuation and, therefore, the extent of outgrowth movement (Figure 1A). In the neuron, this diffusive motion occurs at the micro-scale as innumerable forces act upon the membrane. An increase in diffusive motion at the micro-scale might be observed at the macro-scale as a decrease in the rate of outgrowth.

In this model, guidance cues promote or inhibit outgrowth but they do not intrinsically cause an attractive or repulsive directional response. This is because the direction of outgrowth is determined by a directional bias that is created over time by the combined effect of extracellular cues. In the example illustrated in Figure 2A, a neuronal protrusion experiences an extracellular guidance cue(s) (orange) that is present in a posterior (right) to anterior (left) increasing concentration gradient. This cue acts together with other cues (purple and blue) that set the probability of outgrowth in the dorsal and ventral directions. As long as the probabilities of dorsal and ventral outgrowth are equal, a bias for anterior movement over time is created. For example, at time 1 (Figure 2A top) the probability of anterior outgrowth is 0.8, whereas the probability of dorsal outgrowth is 0.1 and probability of ventral outgrowth is 0.1. As the protrusion travels in the anterior direction it encounters higher levels of the cue. Even if the cue inhibits outgrowth, an anterior directional bias towards the source of that cue can be maintained. For example, at time 2 (Figure 2B bottom), the probability of anterior outgrowth may have been reduced to 0.4 because of the inhibitory effect of the cue. Assuming that signaling mechanisms within the neuron remain relatively constant as the protrusion transverses this environment, the probabilities of dorsal and ventral outgrowth will increase (the sum of the probabilities must equal one because of SOAL). Therefore, the probability of dorsal outgrowth will be 0.3 and the probability of ventral outgrowth will be 0.3 in this example. While this increases the back and forth fluctuation that occurs perpendicular to the

direction of outgrowth, it does not change the directional bias that occurs over time and movement will still be towards the inhibitory cue.

The model makes predictions about patterns of outgrowth in response to extracellular cues. In this example, the neuron's response to the extracellular cues does not have an effect on the directional bias. However, random walk modeling (shown above each diagram and explained in detail later) predicts that a change in the degree to which the direction of outgrowth movement fluctuates will alter the extent of outgrowth. The pattern of outgrowth can be influenced by how great the fluctuation becomes as outgrowth moves towards a source of a cue. For example, if the fluctuation becomes significant as a protrusion moves towards the source, outgrowth will stall before reaching the source. However, if the fluctuation is not great enough at the source of the cue, outgrowth could continue to move forward. This is because the probability of movement in the opposite, inward, direction is low. For instance, a probability of 0.33 anterior, 0.33 dorsal, and 0.33 ventral outgrowth still creates an anterior directional bias. Therefore, in contrast to the attraction and repulsion model, this model does not predict that movement across a source of a cue requires the neuron to switch its responsiveness to the cue.

In the discussion above, a protrusion moves toward the source of an inhibitory cue. However, a similar prediction can be made for movement towards the source of a cue that promotes outgrowth. Assuming that receptor levels at each surface and signaling mechanisms remain relatively constant as the protrusion transverses this environment, the probabilities of dorsal and ventral outgrowth will increase as more receptors at these surfaces are stimulated due to an increasing concentration of the cue. Correspondingly, the probability of outgrowth at the

anterior surface will decrease because of SOAL. As with the case of the inhibitory cue, the result is an increase in the degree to which the direction of outgrowth fluctuates.

The SOAL model makes predictions about how guidance genes might affect outgrowth patterning. The SOAL process allows the direction of outgrowth activity to fluctuate. In Figure 2, the relative degree to which UNC-40-mediated (red) and nonUNC-40-mediated (green) outgrowth activity fluctuates under different circumstances is depicted by the extent to which the colored areas cover the neuron's surface. Extracellular cues can influence the degree to which the direction of outgrowth fluctuates (Figure 2A). Likewise, mutations that disrupt the UNC-40 SOAL process could also change the degree to which the direction of UNC-40-mediated outgrowth fluctuates. By altering the extent of outgrowth movement, these genes could regulate the length of a neuron's extension (Figure 2B). In addition to length, the model predicts that the number of processes may be affected. Since extracellular cues are not uniformly distributed across a neuron's surface, the extent of outgrowth movement could vary along the leading-edge surface of a neuron, leading to multiple outgrowths extending in the same direction. Such phenotypes might not have been associated with guidance genes since most genetic studies have focused on only whether movement is disrupted towards or away from the source of a cue. UNC-5, in particular, has been regarded as the quintessential repulsive guidance receptor and *unc-5* mutations are most often interpreted using this perspective.

Because we observed that UNC-5 affects UNC-40 SOAL (KULKARNI *et al.* 2013), we hypothesized that *unc-5* might regulate the length and number of neuronal processes. Therefore, we decided to look at neuronal outgrowth patterns in *unc-5* mutants for changes in the length and number

of processes. In particular, we focused on outgrowth that was not directed away from UNC-6 sources since the SOAL model predicts that these outgrowth patterns are not caused by a repulsion mechanism and that they should occur independently of the direction of outgrowth. We further reasoned that if *unc-5* regulates this type of patterning then UNC-40 SOAL might be regulated by specific genetic pathways. We therefore asked whether genetic interactions between *unc-5* and other guidance genes can affect UNC-40 SOAL.

In this paper, we present genetic evidence that UNC-5 regulates the length and number of processes that neurons development. We argue that these results can be interpreted using the SOAL model. We also show genetic interactions that suggest the UNC-5 and SAX-3 (Robo) receptors, and the cytoplasmic proteins, UNC-53 (NAV2), MIG-15 (NIK kinase), and MADD-2 (TRIM), function through specific signaling pathways to regulate UNC-40 SOAL in response to the UNC-6 and EGL-20 (wnt) extracellular cues. Together these results suggest that the SOAL model is useful for understanding how genes regulate patterns of outgrowth.

Materials and Methods

Strains

Strains were handled at 20 ℃ using standard methods (Brenner, 1974) unless stated otherwise. A Bristol strain N2 was used as wild type. The following alleles were used: **LGI**, *unc-40(e1430), unc-40(ur304), zdIs5[mec-4::GFP]*; **LGII**, *unc-53(n152)*; **LGIV,** *unc-5(e152), unc-5(e53), unc-5(ev480), unc-5(ev585),egl-20(n585), kyIs262[unc-86::myr-GFP;odr-1::dsRed];* **LGIV,** *madd-2(ky592), madd-2(tr103)*; **LGX**, *mig-15(rh148), unc-6(ev400)*, *sax-3(ky123), sax-3(ky200).* Transgenes maintained as extrachromosomal arrays included: *kyEx1212 [unc-86::unc-40-GFP;odr-1::dsRed].*

Analysis of axon outgrowth and cell body position

HSN neurons were visualized using expression of the transgene *kyIs262[unc-86::myr-GFP].* The mechanosensory neurons, AVM, ALM, and PLM, were visualized using the expression of the transgene *zdIs5[Pmec-4::GFP]*. Synchronized worms were obtained by allowing eggs to hatch overnight in M9 buffer without food. The larval stage was determined by using differential interference contrast (DIC) microscopy to examine the gonad cell number and the gonad size. Staged larvae were mounted on a 5% agarose pad with 10 mM levamisole buffer. Images were taken using epifluorescent microscopy with a Zeiss 63X water immersion objective.

The number of processes during early L1 larval stage was scored by counting the number of processes that extended for a distance greater than the length of one cell body. We report instances in which there were no such processes, one process or more than one processes. In the L2 larval stage, a single early process was scored if there was only one major extension from the ventral leading edge. The HSN cell body in L2 stage larvae was scored as dorsal if the

cell body had failed to migrate ventrally and was not positioned near the PLM axon. In L4 stage larvae, a multiple ventral processes phenotype was scored if more than one major extension protruded from the ventral side of cell body.

Extension into the nerve ring was scored as defective if the axon did not extend further than approximately half the width of the nerve ring. Anterior extension was scored as defective if the axon did not extend further anteriorly than the nerve ring. PLM axons are scored as over-extending if they extended further anterior than the position of the ALM cell body.

Analysis of the direction of HSN outgrowth

HSN was visualized using the transgene *kyIs262[unc-86::myr-GFP].* L4 stage larvae were mounted on a 5% agarose pad with 10 mM levamisole buffer. An anterior protrusion was scored if the axon extended from the anterior side of the cell body for a distance greater than the length of three cell bodies. A dorsal or posterior protrusion was scored if the axon extended dorsally or posteriorly for a distance greater than two cell body lengths. HSN was considered multipolar if more than one process extended a length greater than one cell body. Images were taken using epifluorescent microscopy with a Zeiss 40X objective.

Analysis of the UNC-40::GFP localization in L2 stage animal

For analysis of UNC-40::GFP localization, L2 stage larvae with the transgenic marker *kyEx1212[unc-86::unc-40::GFP; odr-1::dsRed]* were mounted on a 5% agarose pad with 10 mM levamisole buffer. Staging was determined by examining the gonad cell number and the gonad size under differential interference contrast (DIC) microscopy. Images were taken using epifluorescent microscopy with a Zeiss 63X water immersion objective. The UNC-40::GFP

localization was determined by measuring the average intensity under lines drawn along the dorsal and ventral edges of each HSN cell body by using ImageJ software. For analysis of the anterior–posterior orientation of UNC-40::GFP, the dorsal segment was geometrically divided into three equal lengths (dorsal anterior, dorsal central and dorsal posterior segments). The line-scan intensity plots of each of these segments were recorded. ANOVA test was used to determine if there is a significant difference between intensities of the three segments. The dorsal distribution was considered uniform if $p \geq 0.05$ and was considered asymmetrical if $p \leq 0.05$. Within an asymmetric population, the highest percent intensity was considered to localize UNC-40::GFP to either anterior, posterior or central domain of the dorsal surface.

Computations

A program to simulate a two-dimensional lattice random walk based on the probability of dorsal, ventral, anterior, and posterior outgrowth for a mutant (Table 1) was created using MATLAB. (The directions of the axons from multipolar neurons were not scored. These axons appear to behave in the same manner as the axons from monopolar neurons, but this has not yet been tested.) The probability of dorsal, ventral, anterior, or posterior outgrowth was assigned for the direction of each step of a random walk moving up, down, left or right, respectively. Each variable is considered independent and identically distributed. Simulations of 500 equal size steps (size =1) were plotted for 50 tracks (Figure 1B, 5B and 6B inserts). A Gaussian distribution for the final positions of the tracks was generated using Matlab's random function (Figure 6).

The mean squared displacement (MSD) is used to provide a quantitative characteristic of the

motion that would be created by the outgrowth activity undergoing the random walk. Using the random walks generated for a mutant the MSD can be calculated:

$$msd(\tau) = < [r(t + \tau) - \mathrm{r}(t)]^2 >$$

Here, r(t) is the position at time t and τ is the lag time between two positions used to calculate the displacement, Δr(τ) = r(t+τ) - r(t). The time-average over t and the ensemble-average over the 50 trajectories were calculated. This yields the MSD as a function of the lag time. A coefficient giving the relative rate of diffusion was derived from a linear fit of the curve. The first two lag time points were not considered, as the paths often approximate a straight line at short intervals.

Results

UNC-5 regulates the pattern of outgrowth from the HSN neuron

To investigate whether UNC-5 activity can regulate the length or number of processes that a neuron can develop when outgrowth is towards an UNC-6 source, we examined the development of the HSN axon in *unc-5* mutations. The HSN neuron sends a single axon to the ventral nerve cord, which is a source of the UNC-6 cue (WADSWORTH *et al.* 1996; ADLER *et al.* 2006; ASAKURA *et al.* 2007). Axon formation is dynamic (ADLER *et al.* 2006). Shortly after hatching, HSN extends short neurites in different directions. These neurites, which dynamically extend and retract filopodia, become restricted to the ventral side of the neuron where a leading edge forms. Multiple neurites extend from this surface until one develops into a single axon extending to the ventral nerve cord. Measurements of growth cone size, maximal length, and duration of growth cone filopodia indicate that UNC-6, UNC-40, and UNC-5 control the dynamics of protrusion (NORRIS AND LUNDQUIST 2011).

We observe that in *unc-5* mutants, the patterns of extension are altered. In wild-type animals at the L1 stage of development most HSN neurons extends more than one short neurite, however in *unc-5(e53)* mutants nearly half the neurons do not extend a process (Figures 3A and 3B). During the L2 stage in wild-type animals a prominent ventral leading edge forms and the cell body undergoes a short ventral migration that is completed by the L3 stage. By comparison, in *unc-5* mutants the cell body may fail to migrate and instead a single large ventral process may form early during the L2 stage (Figures 3A, 3C and 3E). It may be that the ventral migration of the HSN cell body requires the development of a large leading edge with multiple extensions. Together the observations indicate that loss of *unc-5* function affects the patterning of outgrowth, *i.e.* the timing, length, and number of extensions that form. Loss of *unc-5* function does not prevent movement, in fact, a single large

ventral extension can form in the mutant at a time that is even earlier than when a single ventral extension can be observed in wildtype.

We tested four different *unc-5* alleles in these experiments. The *unc-5(e53)* allele is a putative molecular null allele, *unc-5(ev480)* is predicted to truncate UNC-5 after the cytoplasmic ZU-5 domain and before the Death Domain, *unc-5(e152)* is predicted to truncate UNC-5 before the ZU-5 domain and Death Domain, and *unc-5(ev585)* is a missense allele that affects a predicted disulfide bond in the extracellular Ig(C) domain (KILLEEN *et al.* 2002). Although both the *unc-5(ev480)* and *unc-5(e152)* are predicted to cause premature termination of protein translation in the cytodomain, the *unc-5(e152)* product retains the signaling activity that prevents these phenotypes. Based on other phenotypes, previous studies reported that the *unc-5(e152)* allele retains UNC-40-dependent signaling functions (MERZ *et al.* 2001; KILLEEN *et al.* 2002).

UNC-5 is required for the induction of multiple HSN axons by UNC-6ΔC and a *mig-15* mutation

The results above suggest that UNC-5 activity can regulate the number of HSN extensions that form. To further test this hypothesis, we checked whether loss of UNC-5 function can suppress the development of additional processes that can be induced. Previously we reported that expression of the N-terminal fragment of UNC-6, UNC-6ΔC, induces excessive branching of ventral nerve cord motor neurons and that UNC-5 can suppress this branching (LIM *et al.* 1999). We now report that HSN develops an extra process in response to UNC-6ΔC and that UNC-5 suppresses the development of this extra process (Figures 3D and 3F).

To investigate whether this UNC-5 activity might involve known effectors of asymmetric neuronal outgrowth, we tested for genetic interactions between *unc-5* and both *mig-10* and *mig-15*. MIG-10 (lamellipodin) is a cytoplasmic adaptor protein that can act cell-autonomously to promote UNC-40-mediated asymmetric outgrowth (ADLER *et al.* 2006; CHANG *et al.* 2006; QUINN *et al.* 2006; QUINN *et al.* 2008; MCSHEA *et al.* 2013). MIG-15 (NIK kinase) is a cytoplasmic protein and evidence indicates that *mig-15* functions cell-autonomously to mediate a response to UNC-6 (POINAT *et al.* 2002; TEULIÈRE *et al.* 2011). It's proposed that *mig-15* acts with *unc-5* to polarize the growth cone's response and that it controls the asymmetric localization of MIG-10 and UNC-40 (TEULIÈRE *et al.* 2011; YANG *et al.* 2014). We previously noted that HSN neurons often become bipolar in *mig-15* mutants and frequently UNC-40::GFP is localized to multiple surfaces in a single neuron, suggesting that loss of MIG-15 enhances the ability of UNC-40::GFP to cluster (YANG *et al.* 2014). In our experiments we used the *mig-10 (ct141)* loss-of-function allele (MANSER AND WOOD 1990; MANSER *et al.* 1997) and the *mig-15(rh148)* allele, which causes a missense mutation in the ATP-binding pocket of the kinase domain and is a weak allele of *mig-15* (SHAKIR *et al.* 2006; CHAPMAN *et al.* 2008).

We find that the extra processes induced by UNC-6ΔC expression are suppressed by *mig-10(ct141)* (Figures 3F). We also find that the *mig-15* mutation causes extra HSN processes and that the loss of UNC-5 function suppresses these extra HSN processes (Figures 3F and 3G). These results support the hypothesis that the ability of UNC-5 to regulate the development of multiple protrusions involves the molecular machinery that controls UNC-40-mediated asymmetric neuronal outgrowth.

UNC-5 is required for PLM overextension

The SOAL model predicts that the ability of UNC-5 to regulate the length and number of neural protrusions is independent of the direction of outgrowth. HSN sends a single axon ventrally, while PLM sends an axon anteriorly from a posteriorly positioned cell body. The HSN axon travels towards UNC-6 sources, whereas the PLM axon pathway is perpendicular to UNC-6 sources. To investigate whether UNC-5 activity can regulate the length or number of processes that develop perpendicular to UNC-6 sources we examined the development of the PLM axon. We also chose PLM because UNC-5 is already known to affect the length of the PLM axon. It was previously reported that in *rpm-1* mutants the PLM axon will overextend in the anterior direction and that this phenotype can be suppressed by *sax-3* and *unc-5* loss-of-function mutations (LI *et al.* 2008). In *rpm-1* loss-of-function mutations there is an increase in the level of UNC-5::GFP expression, suggesting that the level of UNC-5 within PLM is important for controlling overextension. However, the overextension in the *rpm-1* mutant is not suppressed by a loss-of-function *unc-40* mutation (LI *et al.* 2008), suggesting that the overextension does not involve UNC-40 SOAL, but rather another outgrowth activity that is nonUNC-40-mediated.

Given that UNC-5 activity is involved in the overextension of the PLM axon, and that the *mig-15* mutation affects HSN outgrowth in an UNC-40 dependent fashion, we decided to test whether PLM overextension might be induced by the *mig-15* mutation in an UNC-40-dependent fashion. The HSN results suggest that altering *mig-15* function creates a sensitized genetic background. That is, the *unc-5(ev480)* mutation suppresses HSN outgrowth extension in both the wild-type and *mig-15(rh148)* backgrounds, but the *mig-15* mutation creates a stronger patterning phenotype. This idea is supported by the evidence that the *mig-15* mutation enhances the ability of UNC-40 to localize at surfaces (YANG *et al.* 2014).

We find that in *mig-15(rh148)* mutants the PLM axon often fails to terminate at its normal position and instead extends beyond the ALM cell body. This overextension is suppressed in *unc-5(e53);mig-15(rh148)* and *unc-40(e1430);mig-15(rh148)* mutants (Figures 4A and 4B). The results are consistent with the idea that UNC-5 is required for the UNC-40-mediated outgrowth activitythat causes overextension in *mig-15(rh148)* mutants.

UNC-5 is required for ALM and AVM branching and extension

We also investigated the effect of UNC-5 activity on patterning where sources of UNC-6 and other cues are in a more complex arrangement. Specifically, we examined whether UNC-5 plays a role in the outgrowth of AVM and ALM processes at the nerve ring. During larval development, processes from the AVM neuron and the two ALM neurons (one on each side of the animal) migrate anteriorly to the nerve ring at dorsal and ventral positions respectively (Figure 4C). At the nerve ring each axon branches; one branch extends further anteriorly and the other extends into the nerve ring. Evidence suggests that at the midbody of the animal the positioning of these axons along the dorsal-ventral axis requires UNC-6, UNC-40, and UNC-5 activity. In *unc-6*, *unc-40,* and *unc-5* null mutants, or when the UNC-6 expression pattern is altered, the longitudinal nerves are mispositioned (REN *et al.* 1999). Glia cells and neurons at the nerve ring are sources of UNC-6 (WADSWORTH *et al.* 1996). The guidance of some axons in the nerve ring are disrupted in *unc-6* and *unc-40* mutants (HAO *et al.* 2001; YOSHIMURA *et al.* 2008). The precise spatial and temporal arrangement of the UNC-6 cue in relationship to the position of the migrating growth cones is not fully understood. Nevertheless, the anteriorly migrating growth cones appear to use the UNC-6 cue from the ventral sources to help maintain the correct dorsal-ventral position, even while moving towards the nerve ring, which is a new source of UNC-6 that is perpendicular to the ventral source. At the nerve ring the axons branch. One process

379 continues anteriorly, moving past the new UNC-6 source, whereas the other projects at a right
380 angle and moves parallel to the new source.

381

382 We find genetic interactions involving *unc-5, unc-40,* and *mig-15* that affect outgrowth
383 patterning of the ALM and AVM extensions at the nerve ring (Figures 4C, 4D, and 4E). In *mig-*
384 *15(rh148);unc-5(e53)* mutants, the AVM axon often fails to extend anteriorly from the branch
385 point and only extends into the nerve ring, or it fails to extend into the nerve ring and only
386 extends anteriorly, or it fails to do both and terminates at this point. In *unc-40(e1430)* mutants,
387 the axon often fails to branch into the nerve ring, although it extends anteriorly. In comparison,
388 in *unc-40(e1430);mig-15(rh148)* mutants more axons extend into the nerve ring. These results
389 suggest that UNC-5 helps regulate UNC-40-mediated outgrowth to pattern the outgrowth at the
390 nerve ring.

391

392 **Interactions between *unc-5* and other genes affect the probability of HSN extension in**
393 **each direction**

394 We hypothesize that there are interactions between *unc-5* and other genes that control the
395 degree to which the direction of outgrowth fluctuates. In the SOAL model, the collective effect
396 of all the cues that promote and inhibit outgrowth set a probability of outgrowth at each
397 surface at each instance of time. As the direction of outgrowth fluctuates over time, a bias is
398 created that determines directionality. Since the direction of outgrowth is stochastically
399 determined, gene activity is not inherently associated with movement in a specific direction.
400 This model differs from the attraction and repulsion model where gene activity is assayed
401 based on direction, *i.e.* the direction of movement relative to the source of a cue. The attraction
402 and repulsion model places genes into attractive or repulsive pathways. We hypothesize that

403 *unc-5* and other genes might instead be ordered into pathways based on how they affect the
404 fluctuation of outgrowth activity.

405

406 Probability distributions for the direction of outgrowth are used to study how genes affect the
407 fluctuation of outgrowth activity. By comparing the distributions created from wild-type and
408 mutant animals, the relative effect that genes have on the fluctuation can be determined. To
409 accomplish this, the direction that the HSN axon initially projects from the cell body is scored
410 (Figure 5A). We reason that the initial development of an axon is the result of the collective
411 impact of all the individual outgrowth movements that take place during the initial formation of
412 the axon. In wildtype, there is a high probability for outgrowth in the ventral direction at each
413 instance of time. As such, there is little fluctuation over time and a strong bias for ventrally
414 directed outgrowth is created. A mutation can cause a lower probability of outgrowth in the
415 ventral direction and a higher probability for outgrowth in other directions. This creates
416 greater fluctuation over time and a weaker bias of ventrally directed outgrowth. For this assay,
417 all the outgrowth movement during the initial axon extension is treated as a single event, *i.e.* the
418 movement of the membrane occurs in a single step from the cell body to a position that is at a
419 set length from the cell body (see Materials and Methods). This step is in the anterior,
420 posterior, dorsal, or ventral direction. Thus, direction is the random variable which takes a
421 value of anterior, posterior, dorsal, or ventral. We can determine the probability of occurrence
422 for each value by scoring many individual animals for each strain.

423

424 Using this assay, we tested for genetic interactions between *unc-5* and four other genes; *elg-20,*
425 *sax-3, madd-2,* or *unc-6.* We have chosen these particular genes because previous observations
426 suggest interactions. 1) EGL-20 (Wnt) is a secreted cue expressed from posterior sources (PAN

427 *et al.* 2006) and it affects to which surface of the HSN neuron the UNC-40 receptor localizes and
428 mediates outgrowth (KULKARNI *et al.* 2013). Based on a directional phenotype, a synergistic
429 interaction between *unc-5* and *egl-20* has been observed. In either *unc-5* or *egl-20* mutants the
430 ventral extension of AVM and PVM axons is only slightly impaired, whereas in the double
431 mutants there is much greater penetrance (LEVY-STRUMPF AND CULOTTI 2014). 2) SAX-3(Robo) is
432 a receptor that regulates axon guidance and is required for the asymmetric localization of UNC-
433 40 in HSN (TANG AND WADSWORTH 2014). Based on a directional phenotype, SAX-3 and UNC-40
434 appear to act in parallel to guide the HSN towards the ventral nerve cord (XU *et al.* 2015). 3)
435 MADD-2 is a cytoplasmic protein of the tripartite motif (TRIM) family that potentiates UNC-40
436 activity in response to UNC-6 (ALEXANDER *et al.* 2009; ALEXANDER *et al.* 2010; HAO *et al.* 2010;
437 MORIKAWA *et al.* 2011; SONG *et al.* 2011; WANG *et al.* 2014). MADD-2::GFP and F-actin colocalize
438 with UNC-40::GFP clusters in the anchor cell (WANG *et al.* 2014). 4) Of course, UNC-6 is an UNC-
439 5 ligand. DCC (UNC-40) and UNC5 (UNC-5) are thought to act independently or in a complex to
440 mediate responses to netrin (UNC-6) (COLAVITA AND CULOTTI 1998; HONG *et al.* 1999; MACNEIL *et*
441 *al.* 2009; LAI WING SUN *et al.* 2011).

442

443 In a test for interaction with *egl-20*, we find that in comparison to *unc-5(e53)* or *egl-20(n585)*
444 mutants, the *unc-5(e53);egl-20(n585)* double mutant have a lower probability for ventral
445 outgrowth and higher probability for outgrowth in other directions (Table 1). This suggests
446 that *unc-5* and *egl-20* may act in parallel to achieve the highest probability for HSN ventral
447 outgrowth, *i.e.* they act to prevent UNC-40-mediated outgrowth from fluctuating in other
448 directions.

449

In a test for interaction with *sax-3,* we find that the probability of outgrowth in each direction in *unc-5(e53);sax-3(ky200)* mutants is similar to the probabilities in *sax-3(ky200)*or *sax-3(ky123)* mutants (Table 1). Given the results with *unc-5* and *egl-20*, we further tested the probability of outgrowth in each direction in *egl-20(n585);sax-3(ky123)* mutants. We find that it is similar to the probabilities in *sax-3(ky200)*or *sax-3(ky123)* mutants (Table 1). The *sax-3(ky123)* allele results in a deletion of the signal sequence and first exon of the gene, whereas sax-3(ky200) contains a missense mutation which is thought to cause protein misfolding and mislocalization at the restrictive temperature (25°C) (ZALLEN *et al.* 1998; WANG *et al.* 2013). The *egl-20(n585);sax-3(ky123)* mutants do not grow well and so it is easier to use the temperature sensitive *sax-3* allele. Together, the results suggest that *sax-3* may be required for both the *unc-5*- and the *egl-20*-mediated activities that allow the highest probability for HSN ventral outgrowth.

In a test for interaction with *madd-2,* we find that the probability of outgrowth in each direction in *unc-5(e53);madd-2(tr103)* mutants is similar to the probabilities in *madd-2(tr103)* mutants (Table 1). There is a higher probability for anterior HSN outgrowth, similar to what is observed in *unc-40(e1430)* mutants. These results suggest that *madd-2* might be required for the *unc-40* outgrowth activity. The probability of outgrowth in each direction in *madd-2(tr103);sax-3(ky123)* mutants is similar to the probabilities in *sax-3(ky200)*or *sax-3(ky123)* mutants (Table 1). The *madd-2(tr103)* allele appears to act as a genetic null (ALEXANDER *et al.* 2010).

In a test for interaction with *unc-6,* we find that the probability of outgrowth in each direction in *unc-5(e53);unc-6(ev400)* and *unc-40(e1430);unc-5(e53)* mutants is similar to the probabilities in *unc-6(ev400)* mutants insofar as there is a lower probability for ventral outgrowth and a higher probability for anterior outgrowth (Table 1). However, the probabilities in each

direction are closer to those obtained from the *unc-40(e1430)* mutants because the probability of anterior outgrowth is lower in these mutants than in *unc-6* mutants. This suggest that UNC-5 and UNC-40 might help increase the probability of anterior outgrowth in the absence of UNC-6.

Taken together, these results support the hypothesis that there are genetic interactions that regulate the degree to which the direction of outgrowth fluctuates. Rather than defining the function of a gene by its ability to control a deterministic event, *i.e.* outgrowth in one direction, gene function can be defined by its ability to control a stochastic process, *i.e.* the probability of outgrowth in different directions.

unc-5 is a member of a class of genes that has a similar effect on the spatial extent of movement

How does *unc-5* affect outgrowth movement? The results above show that *unc-5* and its interactions with other genes affect the degree to which the direction of outgrowth fluctuates. The degree of fluctuation differs depending on the genes involved. The SOAL model predicts that these differences alter the extent of outgrowth; the more the direction of movement fluctuates, the shorter the distance of travel is in a given amount of time.

To depict how *unc-5* and other genes differentially regulate outgrowth movement, we use random walk modeling. Random walks describe movement that occurs as a series of steps in which the angles and the distances between each step is decided according to some probability distribution. By using the probability distribution obtained from a mutant for each step of a random walk, and by keeping the distance of each step equal, a random walk can be constructed (Figure 5A). In effect, this method applies the probability distribution to discrete

particles having idealized random walk movement on a lattice. By plotting random walks derived from wild-type animals and different mutants, the relative effect that mutations have on random walk movement can be visualized. For example, Figure 5B shows 50 tracks of 500 steps for wildtype and two mutants (mutant A is *unc-5(e53)* and mutant B is *egl-20(n585);sax-3(ky123)*). This reveals the effect that a mutation has on the displacement of movement. After 500 steps the displacement from the origin (0,0) is on average less for mutant A than for wildtype, and less for mutant B than for wildtype or mutant A.

The random walk models show the relative effect that a mutation has on a property of outgrowth movement. It is worth noting that this is not modeling the actual trajectory of migrating axons. Neuronal outgrowth is essentially a mass transport process in which mass (the molecular species of the membrane) is sustained at the leading edge and moves outward. Our assay compares the effect that different mutations would have on the movement of mass at the leading edge of an extension if the conditions of the system were kept constant. Of course, *in vivo* the conditions are not constant. For one, as an extension moves it will encounter new environments where the cues may be new or at different concentrations, all of which affect the probability distribution. The actual patterns of outgrowth observed are the result of all the probabilities for outgrowth that occur at each instance of time. It has recently been suggested that our description might be more accurately described as neuro-percolation, a superposition of random-walks (AIELLO 2016).

Our random walk analysis compares the effect that different mutations have on the properties of movement. In wild-type animals, there is a high probability for outgrowth in the ventral direction. The analysis shows that conditions in wildtype create nearly straight-line movement,

i.e. if the same random walk is repeatedly done for the same number of steps, starting at the same origin, the final position of the walk along the x axis does not vary a great amount. In comparison, we find that a mutation can create random walk movement in which the final position is more varied. This variation occurs because the mutation increases the probability of outgrowth in other directions. For each mutation, we simulate 50 random walks of 500 steps and derive the mean and standard deviation of the final position along the X-axis. To compare strains, we plot the normal distribution, setting the mean at the same value for each. The difference between the curve for a mutant and wildtype shows the degree to which the mutation caused the direction of outgrowth to fluctuate (Figure 5C).

The results reveal four different distribution patterns (Figure 6). The first class is the wild-type distribution, which has the distribution curve with the highest peak. The second class comprises *unc-5, egl-20, unc-53,* and *unc-6* in which the distribution curve is flatter than the wild-type curve. We included *unc-53* because our previous study showed that it has genetic interactions with *unc-5* and *unc-6* (KULKARNI *et al.* 2013). The *unc-53* gene encodes a cytoskeletal regulator related to the mammalian NAV proteins and *unc-53* mutations cause guidance defects (MAES *et al.* 2002; STRINGHAM *et al.* 2002; STRINGHAM AND SCHMIDT 2009). The third class has a distribution curve which is flatter than the second and comprises *sax-3, mig-15,* and several double mutation combinations (Figure 6). The fourth class has the flattest distribution curve and comprises *egl-20;sax-3*, *unc-40;sax-3,* and *unc-53;sax-3;unc-6*. This class indicates the greatest degree of fluctuation. The ability to cause the direction of movement to fluctuate is not associated with a specific direction of HSN movement. For example, *unc-5;sax-3, unc-53;unc-6, unc-40;egl-20,* and *madd-2;sax-3* each show a widely dispersed pattern, but the direction is ventral, dorsal, anterior, and posterior, respectively (Figure 6).

The distribution patterns indicate that genes have different effects on the extent that outgrowth movement can travel through the environment. Mean squared displacement (MSD) is a measure of the spatial extent of random motion. The MSD can be calculated from the random walk data. Plotting MSD as a function of the time interval shows how much an object displaces, on average, in a given interval of time, squared (Figure 7A). For normal molecular diffusion, the slope of the MSD curve is directly related to the diffusion coefficient. In cell migration models this value is referred to as the random motility coefficient. Coefficients are experimentally determined; they describe how long it takes a particular substance to move through a particular medium. We determine this value in order to numerically and graphically compare how mutations can alter displacement relative to wildtype (Figure 7B). The four classes of genes are apparent by comparing the height of the bars in Figure 7B.

The results of this modeling suggest that the activities of certain genes, and combinations of genes, have distinct effects on the rate of outgrowth movement. In theory, these differences could be an important means by which genes cause different outgrowth patterns.

unc-5 and other genes regulate UNC-40 receptor clustering, which is a consequence of the SOAL process

How does *unc-5* affect the localization of the UNC-40 receptor and how does this localization affect UNC-40-mediated outgrowth activity and the pattern of outgrowth? Beginning in the early L2 stage, UNC-40::GFP becomes localized to the ventral side of HSN in wildtype (ADLER *et al.* 2006; KULKARNI *et al.* 2013). Reflecting the dynamic morphological changes that occur as the HSN axon forms, the site of asymmetric UNC-40::GFP localization alternates in the neurites and

along the ventral surface of the neuron (KULKARNI *et al.* 2013). Dynamic UNC-40::GFP localization patterns have also been reported for the anchor cell, in which UNC-40 and UNC-6 are also key regulators of extension (ZIEL *et al.* 2009; HAGEDORN *et al.* 2013). Live imaging of the anchor cell reveals that UNC-40::GFP "clusters" form, disassemble, and reform along the membrane (WANG *et al.* 2014). However, live imaging can't directly ascertain whether the position of a cluster is randomly determined since a movement event cannot be repeatedly observed to determine a probability distribution. Mathematical modeling of cluster movement as a stochastic process has not been done. Nevertheless, the results are consistent with the fact that a probability distribution for the direction of UNC-40-mediated HSN outgrowth movement can be determined and, therefore, the UNC-40 localization that gives rise to the outgrowth activity can be defined as a stochastic process.

The UNC-40::GFP clustering phenomena raises questions about the relationship between robust UNC-40 clustering (*i.e.,* sites of distinct UNC-40 localization observable by UNC-40::GFP) and UNC-40-mediated outgrowth activity. Two models are presented in Figure 8. In the first model, the SOAL mechanism causes UNC-40 clustering, which is required for UNC-40-mediated outgrowth activity (Figure 8A). In the second model, SOAL and outgrowth activities are independent and can happen concurrently (Figure 8B). In the first model, the output of the SOAL process is receptor clustering. This is next followed by outgrowth activity from the locations at the membrane where the clusters become stable. This model renders UNC-40-mediated outgrowth a deterministic event occurring at the macro-scale. In the second model, the SOAL process and outgrowth activity are concurrent activities which can occur stochastically along the membrane at the micro-scale. UNC-40 clustering in this model might be an observable consequence of the micro-scale stochastic process that arises over time.

The models make specific predictions that can be tested. In the first model, UNC-40-mediated outgrowth will not happen if UNC-40 does not cluster. In the second model, the loss of UNC-40 clustering does not lead to a loss of UNC-40-mediated outgrowth. We favor the second model. In the *sax-3* mutant there is a large fluctuation in the direction of outgrowth; it is in the third class of mutants (Figures 6 and 7). We previously reported that *sax-3* is required for robust UNC-40::GFP asymmetric localization; in *sax-3* mutants UNC-40::GFP remains uniformly dispersed around the periphery of HSN ((TANG AND WADSWORTH 2014) and Figure 9). Whereas in the *sax-3* mutant there is a ventral bias for outgrowth, in the *unc-40;sax-3* mutant there is not (Figure 6). This suggests that in the *sax-3* mutant there is UNC-40-mediated outgrowth activity that helps create a ventral bias. This is consistent with the second model because UNC-40-mediated outgrowth activity is occurring even when robust UNC-40::GFP is not observed.

We hypothesize that a consequence of the micro-scale SOAL process over time is macro-scale UNC-40 clustering. If so, then *unc-5* activity should affect UNC-40::GFP clustering because it affects the degree to which the direction of UNC-40 receptor localization fluctuates. However, even though there is a higher probability that localization occurs at surfaces other than at the ventral surface, we observe robust asymmetrically localized UNC-40::GFP clustering in *unc-5(e53)* mutants (KULKARNI *et al.* 2013). We speculate that *unc-5(e53),* as well as other gene mutations, do not cause the direction of UNC-40 localization to fluctuate enough to prevent observable UNC-40::GFP clustering. We decided to examine UNC-40::GFP clustering in double mutants to see whether there is an additive effect. In double mutants will the direction of UNC-40 localization fluctuate enough so that UNC-40::GFP clustering cannot be observed in our assay?

We made double mutant combinations between *unc-5*, and *egl-20* or *unc-53.* In *egl-20* and *unc-53* single mutants there is fluctuation in the direction of outgrowth (Figures 6 and 7) and robust asymmetrical UNC-40::GFP localization (Figure 9, *unc-53* results were previously reported (KULKARNI *et al.* 2013)). In comparison to the single mutants, the double mutants all show an increase in the degree to which the direction of outgrowth fluctuates (Figures 6 and 7). Further, in contrast to the single mutants, UNC-40::GFP remains uniformly dispersed around the periphery of HSN in the double mutants (Figure 9). The results suggest a correlation between the degree to which UNC-40-mediated outgrowth activity fluctuates and the ability to detect UNC-40::GFP clustering. This is consistent with the second model (Figure 8). We also observe that in *madd-2(tr103)* mutants the direction of outgrowth fluctuates (Table 1), but unlike *egl-20* and *unc-53* single mutants, there is not robust asymmetrical UNC-40::GFP localization and UNC-40::GFP remains uniformly dispersed (Figure 9). The double mutants, *unc-5;madd-2,* are similar to the single *madd-2* mutant. Similar results are observed with *sax-3* and *unc-5;sax-3* mutants (Figure 9). We hypothesize that in the *madd-2* and *sax-3* mutations the degree to which the direction of UNC-40 localization fluctuates is so great that the *unc-5* mutation makes no difference on the UNC-40::GFP clustering phenotype.

We suggest these results support our model in which UNC-40-mediated outgrowth is an independent process that is coupled to the SOAL process in the HSN neuron. Previously we hypothesized that UNC-40 SOAL is a general cellular process that polarizes and orients cellular activities to the surrounding environment (YANG *et al.* 2014). In neurons during the development of axons, UNC-40 SOAL is coupled to the outgrowth machinery. However, UNC-40 SOAL may also become coupled to other cellular activities. For example, UNC-6, UNC-5, and

641 UNC-40 are also known to play a role in localizing synapses in neurons (COLON-RAMOS *et al.*
642 2007; POON *et al.* 2008; KILLEEN 2009).

643

644 **Discussion**

645 In this paper, we show that UNC-5 regulates the number and length of neuronal processes that
646 a neuron can develop. We observe that *unc-5* loss-of-function mutations inhibit the
647 development of multiple neurites during early outgrowth from HSN. They also suppress the
648 development of extra HSN processes that are induced by a *mig-15* mutation or by expression of
649 the N-terminal fragment of UNC-6. We also observe that *unc-5* mutations suppress the anterior
650 overextension of the PLM axon that occurs in the *mig-15* mutant. Finally, in combination with
651 the *mig-15* mutation, *unc-5* loss-of-function mutations affect the branching and extension of
652 ALM and AVM axons at the nerve ring. In each of these cases, the pattern of outgrowth is
653 altered by loss of UNC-5 function. We further show that UNC-5 acts together with UNC-6, EGL-
654 20, SAX-3, UNC-53, MIG-15, and MADD-2 to regulate UNC-40 asymmetric localization at a
655 surface of HSN. Here we discuss a model to explain how UNC-5 could control patterns of
656 outgrowth by regulating UNC-40 stochastically orientated asymmetric localization (SOAL).

657

658 **UNC-40 SOAL; a model to explain *unc-5* phenotypes**

659 We hypothesize that UNC-40 undergoes stochastically orientated asymmetric localization
660 (SOAL) within neurons. Because this is a stochastic process, there is a probability of UNC-40
661 localizing and mediating outgrowth at each surface of the neuron. The probability of outgrowth
662 at each point along a surface may vary. This means that at one instance of time there is a
663 probability that UNC-40-mediated outgrowth will occur in a specific direction from a point
664 along the surface of the neuron. At the next instance of time there is a probability that

outgrowth will not occur at this point, but will instead occur at another point and in a different direction. When considered over time, the direction of outgrowth fluctuates. This type of movement can be modeled as a random walk, and random walks predict that the displacement of the membrane will depend on the degree to which the direction of outgrowth movement fluctuates. Extracellular cues, and the neuron's response to these cues, set the probability of outgrowth happening at each point along the surface and therefore regulate the amount of fluctuation. The process occurs at the micro-scale and it controls the direction and rate of outgrowth movement. Below we describe how this model can explain the patterns of outgrowth extension seen in the *unc-5* mutants.

Figure 2 depicts the essential concepts underlying the explanations. The same depiction is used to explain the mutant phenotypes in Figures 10-15. Four important concepts are presented by these figures. (1) There are numerous extracellular cues acting on the neuron to set the probability of outgrowth in each direction. These cues include secreted molecules, such as UNC-6 and EGL-20, as well as many other cues, such as extracellular matrix components (YANG *et al.* 2014). For movement in the anterior and posterior directions, the neuron's response to the cues sets an equal probability for movement in the dorsal and ventral direction. For movement in the dorsal and ventral directions, the neuron's response to the cues sets an equal probability for movement in the anterior and posterior direction. These cues are depicted in the figures as purple, blue, orange, and red color gradients. (2) Besides UNC-40-mediated outgrowth activity, cues also set the probability of nonUNC-40-mediated outgrowth activity at each surface of the neuron. For example, there is a high probability for anteriorly directed outgrowth in *unc-40* mutants, indicating that the cues set a high probability for anterior nonUNC-40-mediated activity in the mutants. In the figures, a high relative probability for UNC-40-mediated or nonUNC-40-mediated outgrowth activity at a surface is depicted as red

and green areas, respectively. The colored area is concentrated when there is a high probability for outgrowth in one direction, and the area is more diffuse when the probability for outgrowth in directions perpendicular to the directional bias are greater. (3) As the probability of outgrowth decreases in the direction of outgrowth, and the probability of outgrowth in directions perpendicular to the directional bias become greater, the extent of movement forward decreases. This idea is based on random walk modeling. Representative modeling is shown above or to the side of each diagram. 50 random walks from a point on a line were calculated based on the given probabilities. As the probability for movement in directions perpendicular to the directional bias become greater, the extent of movement from the origin decreases. Similarly, we hypothesize that the forward displacement of the membrane decreases as the probability for perpendicular outgrowth movement become greater at the surface of the neuronal membrane. (4) Loss of UNC-5 function causes a higher probability of UNC-40 mediating outgrowth in directions perpendicular to the directional bias. Loss of MIG-15 reduces the probability of UNC-40-mediated outgrowth in directions perpendicular to the directional bias. These ideas are based on our observations of the effects that *unc-5* and *mig-15* mutations have on HSN localization of UNC-40::GFP and the direction of HSN outgrowth. We further speculate that loss of MIG-15 function increases the probability of nonUNC-40-mediated outgrowth in directions perpendicular to the directional bias. This is based on our observation that HSN tends to be bipolar in the *mig-15* mutant (YANG *et al.* 2014), suggesting that nonUNC-40-mediated outgrowth activity, which drives outgrowth anteriorly in other mutants, becomes ineffectual.

PLM extension phenotype: We hypothesize that there is high probability for anteriorly directed outgrowth from the PLM cell body because of the strong effect of a cue(s) which inhibits outgrowth activity and is present in high concentration posterior to the cell body

(Figure 10A, position 1). Dorsal and ventral cues create an equal probability for dorsal and ventral outgrowth, allowing the UNC-40 SOAL process to cause a high probability for anterior outgrowth activity (Figure 10B, position 1). At a position that is further anterior (Figure 10A, position 2), the inhibitory effect of another cue reduces the probability for anterior outgrowth activity, while increasing the probability of outgrowth in the dorsal and ventral directions. This does not affect the anterior bias for outgrowth, although it may affect the rate of outgrowth (Figure 10B, position 2). Cues at an anterior position (Figure 10A, position 3), strongly inhibit outgrowth and cause a greater probability of outgrowth in the dorsal and ventral directions (Figure 10B, position 3). This arrests forward outgrowth. However, in some mutants the inhibitory effect of these cues is not as great, allowing a stronger anterior bias at position 3. As the outgrowth passes this position (Figure 10A, position 4), a situation similar to position 1 is reestablished (Figure 10B, position 4).

We propose that PLM termination and overextension is influenced by the degree to which UNC-40-mediated outgrowth fluctuates at position 3 (Figure11). In wildtype, the cues cause the direction of both UNC-40-mediated and nonUNC-40-mediated outgrowth to fluctuate, resulting in outgrowth stalling. Loss of UNC-40 function will not alter this. Loss of MIG-15 function increases the probability of anterior UNC-40-mediated outgrowth by decreasing the degree to which the direction of UNC-40-mediated outgrowth fluctuates. This allows a stronger anterior directional bias, which results in the overextension phenotype. Loss of UNC-5 suppresses the overextension caused by loss of MIG-15 function by increasing the degree to which the direction of UNC-40-mediated outgrowth fluctuates, reverting the state back towards wildtype.

ALM and AVM nerve ring branching and extension phenotype: We hypothesize that at the nerve ring there are cues, including UNC-6, that are arranged along the dorsal/ventral axis. These cues can promote ALM and AVM axon outgrowth. As an extension nears the nerve ring, these cues help create a high probability for anterior outgrowth (Figure 12A and 12B, position 1). At the nerve ring, the cues create an equal probability for anterior outgrowth and outgrowth into the ring (Figure 12A and 12B, position 2). Outgrowth extends into the nerve ring because the cues of the nerve ring promote outgrowth and because the cues anterior and posterior to the ring set an equal probability of outgrowth in those directions (Figure 12A and 12B, position 3). Outgrowth can also extend anteriorly from the nerve ring if cues anterior to position 2 also promote outgrowth and cues dorsal and ventral create an equal probability of outgrowth in those directions (Figure 12A and 12B, position 4).

We propose that ALM and AVM nerve ring branching and extension at the nerve ring is influenced by the degree to which UNC-40-mediated outgrowth fluctuates at position 2 (Figure 13). In wildtype, the nerve ring cues create a higher probability for UNC-40-mediated outgrowth into the nerve ring. In UNC-40 mutants, the axons often fail to branch into the nerve ring but they still project further anterior, suggesting that the probability for anterior nonUNC-40-mediated outgrowth is high in the *unc-40* mutant. Loss of MIG-15 function does not affect the branching and extension because the higher probability for UNC-40-mediated outgrowth activity remains. In *unc-40;mig-15* mutants, there is extension in both directions because loss of MIG-15 function increases the probability of nonUNC-40-mediated outgrowth in other directions and the nonUNC-40-mediated outgrowth allows outgrowth into the nerve ring. In *unc-5;mig-15* mutants, the direction of both UNC-40-mediated and nonUNC-40-mediated outgrowth fluctuate, causing outgrowth stalling in each direction. In these mutants, there is often an absence of extension both anteriorly and into the nerve ring.

764

765 **HSN extension phenotypes:** We hypothesize that there is high probability for ventrally
766 directed outgrowth from the HSN cell body because of the strong outgrowth-promoting effect
767 of the UNC-6 cue, which is in a higher concentration ventral of the cell body (Figure 14A,
768 position 1). Anterior and posterior cues create an equal probability for anterior and posterior
769 outgrowth, and there is a high probability for ventral outgrowth activity. As an extension
770 moves ventrally it encounters higher levels of the UNC-6 cue. The probability of outgrowth
771 towards the UNC-6 source increases, while the probabilities of outgrowth in the anterior and
772 posterior decrease (Figure 14B, positions 2). However, as the level of UNC-6 saturates the
773 receptors the probability for outgrowth in different directions increases, causing outward
774 movement to stall (Figure 14B, positions 3). The distance from the source of the cue at which
775 this happens is a function of the concentration of the cues, and the cell's ability to interact and
776 respond to the cues. If the cell's response to the UNC-6 cue causes a lower probability of
777 ventral outgrowth than in wildtype, the probabilities of anterior and posterior outgrowth will
778 be greater (Figure 14B, positions 1, right column). The greater fluctuation will slow the rate of
779 outgrowth as extension proceeds (Figure 14B, positions 2, right column). Again, at the source
780 of the cue the response may become saturated and outward movement will stall (Figure 14B,
781 positions 3, right column). In this scenario, the rate of outgrowth decreases, while the direction
782 of outgrowth is the same.

783

784 We propose that HSN extension is influenced by the degree to which UNC-40-mediated
785 outgrowth fluctuates. In wildtype, UNC-40-mediated outgrowth creates a high probability for
786 the initial ventral outgrowth (Figure 15A, top). Loss of UNC-5 function causes a higher
787 probability of UNC-40 mediating outgrowth in the anterior and posterior directions, and

788 consequently a decrease in the rate of outgrowth (Figure 15A, second from top). We suggest
789 this underlies the observation that extensions fail to form in the L1 stage in *unc-5* mutants, but
790 do form over time, and in the same direction, as in wild-type animals.

791

792 We also propose that controlling the degree to which the direction of UNC-40-mediated
793 outgrowth fluctuates at points along the surface can regulate the number of processes that
794 form. We suggest that UNC-40 (DCC), UNC-5 (UNC5), and UNC-6 (netrin) are part of an activator-
795 inhibitor system (GIERER AND MEINHARDT 1972; MEINHARDT AND GIERER 2000). In an activator-
796 inhibitor system two substances act on each other. The activator stimulates its own production as
797 well as produces an inhibitor that can repress the production of the activator. The inhibitor is able to
798 diffuse more rapidly than the activator, which causes patterns of varying concentrations of activator
799 and inhibitor. Pattern formation through local symmetry breaking, signal amplification, and long-
800 range inhibition may involve chemical, mechanical, or coupled mechanochemical processes
801 (GOEHRING AND GRILL 2013).

802

803 We suggest an activator-inhibitor system in which UNC-40 and UNC-5 are the two substances
804 that interact with each other (Figure 15B). This is consistent with evidence indicating that
805 Netrin-1 binds simultaneously to two DCC (UNC-40) molecules or an UNC5/DCC complex (FINCI
806 *et al.* 2014). In the context of an activator-inhibitor system, UNC-5 signaling acts as an activator
807 and UNC-40 signaling acts as an inhibitor. The activator and inhibitor activities "diffuse" at
808 different rates because recruitment of UNC-40 and UNC-5 to the plasma membrane occurs at
809 different rates. This idea is consistent with imaging experiments of cells in culture which
810 suggest that netrin-1 (UNC-6) regulates the distribution of DCC (UNC-40) and UNC5B (UNC-5)
811 at the plasma membrane (GOPAL *et al.* 2016). In these studies, netrin-1 (UNC-6) was shown to
812 stimulate translocation of DCC (UNC-40) and UNC5B (UNC-5) receptors from intracellular

vesicles to the plasma membrane and, further, the transported receptors were shown to localize at the plasma membrane (GOPAL *et al.* 2016).

We propose that signaling by UNC-6-ligated UNC-40 causes outgrowth activity and stimulates translocation of UNC-40 to the site (Figure 15B, step 1). If the outgrowth reaches a critical level of UNC-6 (Figure 15B, step 2), changes to the UNC-6/UNC-40/UNC-5 receptor complexes increase UNC-5 signaling. UNC-5 signaling inhibits UNC-40 translocation to the site and increases the relative levels of UNC-5 (short-range autocatalytic). Locally, UNC-40-mediated outgrowth activity becomes more dispersed, resulting in a slower rate of outgrowth. As UNC-40 translocation to the leading edge is inhibited, the relative levels of UNC-40 at flanking surfaces increases (Figure 15B, step 3). These UNC-40 levels inhibit UNC-5 signaling (long-range inhibition) and prevent the dispersion of UNC-40-mediated outgrowth activity, resulting in a faster rate of outgrowth at the flanking surfaces. In the context of an activator-inhibitor system, UNC-5 signaling functions as an activator because it stimulates its own activity by decreasing the ratio of UNC-40 to UNC-5 at the site of UNC-5 signaling. It also stimulates production of UNC-40 UNC-5-inhibitory activity by increasing the ratio of UNC-40 to UNC-5 at the flanking regions. As the flanking regions move further outward due to the UNC-40-mediated outgrowth activity, UNC-40 translocation to the surface is further stimulated by increasing levels of the extracellular UNC-6 cue.

In this type of model, the reaction and diffusion rates of the substances influence the pattern that emerges. In the above example, whether the flanking areas branch further depends on whether the critical level of receptors and extracellular ligands is realized at the flanking region. The *mig-15(rh148)* mutation and the expression of UNC-6ΔC could alter the rate by which components of the UNC-6/UNC-40/UNC-5 receptor complexes interact or could alter the

838 rate of translocation of the components to the membrane, or both. In fact, cell culture
839 experiments suggest Netrin VI-V (UNC-6ΔC) induces DCC and UNC5B colocalization, but not
840 DCC recruitment (GOPAL *et al.* 2016). Moreover, mutations that suppress ectopic branching
841 induced by UNC-6ΔC expression affect members of second messenger systems which could
842 influence the rates of UNC-40 and UNC-5 interactions and trafficking (WANG AND WADSWORTH
843 2002).

844

845 **A genetic pathway for UNC-40 asymmetric localization**

846 We present a genetic pathway for the asymmetrical localization of UNC-40 based on the phenotype
847 of robust UNC-40::GFP clustering in HSN. It is worth noting that the SOAL model of axon
848 outgrowth does not depend on knowledge of the molecular mechanisms of outgrowth. Rather,
849 the SOAL model uses a statistical approach to understand how a gene influences the collective
850 impact of all the underlying molecular mechanisms that drives outgrowth. It can be envisioned
851 that the movement of an extension occurs through innumerable forces acting at the molecular
852 level. The effect that each molecular event has on movement is not easily observed or
853 measured. In fact, it may be that patterns of outgrowth can't be fully understood by only
854 knowing the molecular mechanisms of outgrowth. Instead, the effects that molecular events
855 collectively have on movement must be understood through a statistical model.

856

857 Nevertheless, a full understanding of the molecular mechanisms underlying the SOAL process is
858 an important long-term goal. Since we believe that UNC-40::GFP clustering is a readout of that
859 process, constructing genetic pathways for the clustering of UNC-40::GFP is a step toward this
860 goal. We wish to know how UNC-5 mediates signaling within HSN that controls the UNC-40
861 asymmetric localization process. However, a role for UNC-5 in HSN is paradoxical given the

862 widespread idea that UNC-5 mediates a repulsive response to UNC-6 and that HSN outgrowth is
863 towards the source of UNC-6. All the same, we suggest a cell-autonomous role for UNC-5 in
864 HSN is the most parsimonious model. First, UNC-5 is an UNC-6 receptor that can mediate
865 neuronal responses when in complex with UNC-40 (HONG *et al.* 1999; GEISBRECHT *et al.* 2003;
866 KRUGER *et al.* 2004; FINCI *et al.* 2014). We previously showed that UNC-40 conformational
867 changes regulate HSN asymmetric localization in HSN (XU *et al.* 2009) and we now show that
868 UNC-5 regulates UNC-40 asymmetric localization in HSN. It is therefore plausible that UNC-5
869 affects UNC-40 conformational changes that regulate UNC-40 asymmetric localization. Second,
870 UNC-5 can alter the number to HSN outgrowths in response to UNC-6 and to the UNC-6ΔC
871 ligand. Directional guidance by UNC-6 and UNC-6ΔC is generally normal in an *unc-5* mutant,
872 suggesting that the ability of UNC-5 to regulate the number of outgrowth is not due to an
873 alteration in the extracellular distribution of its UNC-6 ligand. Further, the UNC-6ΔC ligand and
874 the *mig-15* mutation create the same outgrowth phenotype, which can be suppressed by loss of
875 UNC-5 function, and we have shown that MIG-15 acts cell autonomously in HSN to regulate
876 UNC-40 asymmetric localization (YANG *et al.* 2014). Further, we have shown that the UNC-5-
877 mediated response that regulates UNC-40 asymmetric localization also depends on UNC-53
878 (NAV2) (KULKARNI *et al.* 2013), a cytoplasmic protein that functions cell-autonomously for cell
879 migration and axon guidance (STRINGHAM *et al.* 2002). Together, these observations strongly
880 suggest that UNC-5 directly regulates signaling within HSN. Third, a role for UNC-5 in the
881 guidance of AVM and PVM axons towards UNC-6 sources has also been suggested. A synergistic
882 interaction between *unc-5* and *egl-20* is observed; in either *unc-5* or *egl-20* mutants the ventral
883 extension of AVM and PVM axons is only slightly impaired, whereas in the double mutants
884 there is a much greater penetrance (LEVY-STRUMPF AND CULOTTI 2014). The expression of an *unc-*
885 *5* transgene in AVM and PVM can rescue the AVM and PVM axon guidance defects of the *unc-*
886 *5;egl-20* double mutant (LEVY-STRUMPF AND CULOTTI 2014). We note that for HSN, transgenic

887 rescue using *unc-5* constructs have not been successful and in wild-type animals UNC-5
888 expression in HSN has not been reported. As well, expression has not been reported in AVM,
889 PVM, and PLM wild-type neurons. We suspect there may be technical difficulties or that UNC-5
890 expression might be low in these cells. UNC-5 is detected in PLM in *rpm-1* mutants, which is
891 consistent with evidence that UNC-5 activity is required for PLM overextension in these
892 mutants (Li *et al.* 2008).

893

894 To construct genetic pathways, we use the readout of whether UNC-40::GFP is clearly and
895 consistently localized to any side of the HSN neuron in different mutants (Figure 9). A
896 summary of the results is presented (Figure 16A). UNC-6 is required for robust asymmetric
897 UNC-40 localization; in the absence of UNC-6 function UNC-40 remains uniformly distributed
898 along the surface of the plasma membrane. The loss of both UNC-53 and UNC-5 function also
899 results in a uniform distribution, however loss of either one alone does not. This suggests that
900 UNC-53 and UNC-5 pathways act redundantly downstream of UNC-6 (Figure 16B). Moreover,
901 we observe there is robust asymmetric UNC-40 localization when there is a loss of UNC-6
902 activity in addition to the loss of UNC-53 and UNC-5. This suggests a third pathway that is
903 suppressed by UNC-6 when UNC-53 and UNC-5 activity are missing. Loss of both UNC-5 and
904 UNC-6 does not allow UNC-40 localization, whereas loss of both UNC-53 and UNC-6 does,
905 therefore UNC-53, rather than UNC-5, acts with UNC-6 to suppress the third pathway.

906

907 UNC-40 becomes localized when EGL-20 activity is lost. As well, UNC-40 becomes localized
908 when both EGL-20 and UNC-53 activities are lost. This is consistent with UNC-6 promoting
909 UNC-40 localization via the UNC-5 pathway. Loss of EGL-20 and UNC-5 prevents UNC-40
910 localization. In these animals, the UNC-5 pathway is absent and UNC-6 is present to blocks the

911 third pathway, therefore the UNC-53 pathway that leads to UNC-40 localization must require
912 EGL-20, as well as UNC-6.

913

914 Loss of UNC-6 activity or loss of both UNC-6 and EGL-20 activity prevents localization, whereas
915 loss of only EGL-20 does not. To explain this, we propose that when UNC-6 is lost, the third
916 pathway, which would otherwise be activated by the loss of UNC-6, remains suppressed
917 because EGL-20 activity promotes suppression via UNC-53 activity. This suppression also
918 explains why loss of UNC-6 and UNC-5 activity does not cause localization.

919

920 Importantly, this genetic analysis indicates that netrin (UNC-6) and wnt (EGL-20) signaling are
921 integrated to regulate self-organizing UNC-40 asymmetric localization. An implication of this
922 result is that the extracellular concentrations of UNC-6 and EGL-20 could control the activation
923 or inhibition of UNC-40-mediated outgrowth. This could be important for generating patterns
924 of outgrowth when neurons move to new locations within the animal. The picture is
925 complicated by the evidence that both UNC-6 and EGL-20 affect the SOAL of both UNC-40-
926 mediated and nonUNC-40-mediated outgrowth activity. It is possible that overlapping sets of
927 extracellular cues and their receptors are involved in setting the probability of outgrowth for
928 each activity. SAX-3 and MADD-2 are required for UNC-40::GFP localization, but also affect
929 nonUNC-40-mediated outgrowth. The *egl-20;sax-3* and *unc-40;sax-3* double mutations have the
930 greatest effect on restricting the extent of outgrowth movement in any direction (Figures 6 and
931 7). Moreover, the number of HSN neurites is reduced in *unc-5* mutants, whereas the number in
932 *unc-5;sax-3* double mutants appears normal (Figure 3B). Understanding the interdependence
933 of these outgrowth activities will be necessary for better understand how extracellular cues
934 affect the patterns of outgrowth *in vivo*.

935

Acknowledgments

We thank Caenorhabditis Genetics Center, J. Culotti, and C. Bargmann for strains; we thank Martha Soto and members of the Soto laboratory for support and helpful discussions; we thank Bhumi Patel and Leely Rezvani for comments on the manuscript. This work was supported by grants NS033156 and NS061805 from the National Institutes of Health, National Institute of Neurological Disorders and Stroke and grant 07-3060-SCR-E-0 from the New Jersey Commission on Spinal Cord to WGW. This work was also supported by grant DFHS13PPCO28 from the New Jersey Commission on Cancer Research to AM.

944 # Table

945

946

Table 1. Direction of Axon Formation from the HSN Cell Body

	direction of axon protrusion						
	dorsal	ventral	anterior	posterior	multipolar		
	%	%	%	%	%	*n*	reference
wildtype	0	96±2	3±2	0	1±1	221	(KULKARNI *et al.* 2013)
unc-6(ev400)	2±2	3±2	81±2	8±2	6±1	218	(KULKARNI *et al.* 2013)
unc-40(e1430)	2±1	6±2	67±2	19±1	6±1	183	(KULKARNI *et al.* 2013)
unc-5(e53)	0	75±3	19±2	1±1	5±1	245	(YANG *et al.* 2014)
unc-53(n152)	0	67±3	22±2	5±1	6±1	238	(KULKARNI *et al.* 2013)
sax-3(ky123)	2±1	31±1	21±1	37±2	9±2	232	(TANG AND WADSWORTH 2014)
*sax-3(ky200)**	2±1	32±1	19±2	42±3	5±2	198	(TANG AND WADSWORTH 2014)
unc-5(e53);sax-3(ky200)	2±1	40±3	24±2	28±2	6±1	120	
unc-5(e53);unc-6(ev400)	4±2	5±3	59±4	22±4	9±1	201	
unc-5(e53);egl-20(n585)	3±1	28±4	22±4	35±5	11±2	114	
unc-53(n152);unc-5(e53)	0	19±1	62±2	17±1	3±1	224	(KULKARNI *et al.* 2013)
unc-53(n152);unc-6(ev400)	24±2	0	19±2	22±2	34±3	144	(KULKARNI *et al.* 2013)
unc-53(n152);sax-3(ky123)	1±1	47±3	24±2	23±5	6±3	207	(TANG AND WADSWORTH 2014)
unc-40(e1430);unc-5(e53)	5±1	6±1	55±2	19±2	14±1	196	(KULKARNI *et al.* 2013)
*unc-40(e1430);sax-3(ky200)**	14±3	2±1	40±2	35±3	9±4	191	(TANG AND WADSWORTH 2014)
sax-3(ky200); unc-6(ev400)*	8±1	8±2	49±3	20±5	14±2	211	(TANG AND WADSWORTH 2014)
unc-53(n152);unc-5(e53);unc-6(ev400)	23±2	0	34±2	15±2	28±2	148	(KULKARNI *et al.* 2013)
unc-53(n152);sax-3(ky200);unc-6(ev400)*	11±2	2±1	33±4	30±3	25±5	189	
egl-20(n585)	0	64±2	21±2	7±1	8±1	304	(TANG AND WADSWORTH 2014)
egl-20(n585); unc-6(ev400)	18±2	0	43±2	15±2	24±2	205	(TANG AND WADSWORTH 2014)
unc-40(e1430); egl-20(n585)	6±2	17±2	45±5	15±2	16±2	173	(TANG AND WADSWORTH 2014)
egl-20(n585);sax-3(ky123)	1±1	12±2	39±2	39±1	8±3	177	(TANG AND WADSWORTH 2014)
madd-2(tr103)	0	19±2	55±5	17±4	8±2	179	
madd-2(ky592)	0	52±2	43±2	5±1	0	95	
unc-5(e53);madd-2(tr103)	3±1	15±2	52±4	17±4	13±1	197	
madd-2(tr103);sax-3(ky123)	2	24±3	19±4	47±1	7±2	171	
unc-53(n152);madd-2(tr103)	1±1	15±2	43±2	17±1	24±4	148	
mig-15(rh326)	2±1	15±1	24±3	11±3	48±8	131	(YANG *et al.* 2014)

Numbers represent percentage value ± SEM.

*Animals grown at the *sax-3(ky200)* restrictive temperature (25°C).

947

948 ## References

949 Adler, C. E., R. D. Fetter and C. I. Bargmann, 2006 UNC-6/Netrin induces neuronal asymmetry and
950 defines the site of axon formation. Nat Neurosci 9**:** 511-518.

951 Aiello, G. L., 2016 Neuro-Percolation as a Superposition of Random-Walks, pp. in *European*
952 *Symposium on Artificial Neural Networks, Computational Intelligence and Machine Learning*.
953 i6doc.com Bruges, Belgium.

954 Alexander, M., K. K. Chan, A. B. Byrne, G. Selman, T. Lee *et al.*, 2009 An UNC-40 pathway directs
955 postsynaptic membrane extension in Caenorhabditis elegans. Development 136**:** 911-922.

956 Alexander, M., G. Selman, A. Seetharaman, K. K. Chan, S. A. D'Souza *et al.*, 2010 MADD-2, a
957 homolog of the Opitz syndrome protein MID1, regulates guidance to the midline through UNC-40 in
958 Caenorhabditis elegans. Developmental Cell 18**:** 961-972.

959 Asakura, T., K. Ogura and Y. Goshima, 2007 UNC-6 expression by the vulval precursor cells of
960 Caenorhabditis elegans is required for the complex axon guidance of the HSN neurons. Dev Biol
961 304**:** 800-810.

962 Chan, S. S., H. Zheng, M. W. Su, R. Wilk, M. T. Killeen *et al.*, 1996 UNC-40, a C. elegans homolog
963 of DCC (Deleted in Colorectal Cancer), is required in motile cells responding to UNC-6 netrin cues.
964 Cell 87**:** 187-195.

965 Chang, C., C. E. Adler, M. Krause, S. G. Clark, F. B. Gertler *et al.*, 2006 MIG-10/Lamellipodin and
966 AGE-1/PI3K Promote Axon Guidance and Outgrowth in Response to Slit and Netrin. Curr Biol 16**:**
967 854-862.

968 Chapman, J. O., H. Li and E. A. Lundquist, 2008 The MIG-15 NIK kinase acts cell-autonomously in
969 neuroblast polarization and migration in C. elegans. Dev Biol 324**:** 245-257.

970 Colavita, A., and J. G. Culotti, 1998 Suppressors of ectopic UNC-5 growth cone steering identify
971 eight genes involved in axon guidance in Caenorhabditis elegans. Dev Biol 194**:** 72-85.

972 Colon-Ramos, D. A., M. A. Margeta and K. Shen, 2007 Glia promote local synaptogenesis through
973 UNC-6 (netrin) signaling in C. elegans. Science 318**:** 103-106.

974 Finci, L. I., N. Krüger, X. Sun, J. Zhang, M. Chegkazi *et al.*, 2014 The crystal structure of netrin-1 in
975 complex with DCC reveals the bifunctionality of netrin-1 as a guidance cue. Neuron 83**:** 839-849.

976 Geisbrecht, B. V., K. A. Dowd, R. W. Barfield, P. A. Longo and D. J. Leahy, 2003 Netrin binds
977 discrete subdomains of DCC and UNC5 and mediates interactions between DCC and heparin. J Biol
978 Chem 278**:** 32561-32568.

979 Gierer, A., and H. Meinhardt, 1972 A theory of biological pattern formation. Kybernetik 12**:** 30-39.

980 Goehring, N. W., and S. W. Grill, 2013 Cell polarity: mechanochemical patterning. Trends Cell Biol
981 23**:** 72-80.

982 Gopal, A. A., B. Rappaz, V. Rouger, I. B. Martyn, P. D. Dahlberg *et al.*, 2016 Netrin-1-Regulated
983 Distribution of UNC5B and DCC in Live Cells Revealed by TICCS. Biophys J 110**:** 623-634.

984 Hagedorn, E. J., J. W. Ziel, M. A. Morrissey, L. M. Linden, Z. Wang *et al.*, 2013 The netrin receptor
985 DCC focuses invadopodia-driven basement membrane transmigration in vivo. J Cell Biol 201**:** 903-
986 913.

987 Hao, J. C., C. E. Adler, L. Mebane, F. B. Gertler, C. I. Bargmann *et al.*, 2010 The tripartite motif
988 protein MADD-2 functions with the receptor UNC-40 (DCC) in Netrin-mediated axon attraction and
989 branching. Dev Cell 18**:** 950-960.

990 Hao, J. C., T. W. Yu, K. Fujisawa, J. G. Culotti, K. Gengyo-Ando *et al.*, 2001 C. elegans Slit Acts in
991 Midline, Dorsal-Ventral, and Anterior-Posterior Guidance via the SAX-3/Robo Receptor. Neuron 32**:**
992 25-38.

993 Hedgecock, E. M., J. G. Culotti and D. H. Hall, 1990 The unc-5, unc-6, and unc-40 genes guide
994 circumferential migrations of pioneer axons and mesodermal cells on the epidermis in C. elegans.
995 Neuron 4**:** 61-85.

996 Hong, K., L. Hinck, M. Nishiyama, M. M. Poo, M. Tessier-Lavigne *et al.*, 1999 A ligand-gated
997 association between cytoplasmic domains of UNC5 and DCC family receptors converts netrin-
998 induced growth cone attraction to repulsion. Cell 97**:** 927-941.

999 Keleman, K., and B. J. Dickson, 2001 Short- and long-range repulsion by the Drosophila Unc5 netrin
1000 receptor. Neuron 32**:** 605-617.

1001 Killeen, M., J. Tong, A. Krizus, R. Steven, I. Scott *et al.*, 2002 UNC-5 function requires
1002 phosphorylation of cytoplasmic tyrosine 482, but its UNC-40-independent functions also require a
1003 region between the ZU-5 and death domains. Dev Biol 251**:** 348-366.

1004 Killeen, M. T., 2009 The dual role of the ligand UNC-6/Netrin in both axon guidance and
1005 synaptogenesis in C. elegans. Cell Adh Migr 3**:** 268-271.

Kruger, R. P., J. Lee, W. Li and K. L. Guan, 2004 Mapping netrin receptor binding reveals domains of Unc5 regulating its tyrosine phosphorylation. J Neurosci 24**:** 10826-10834.

Kulkarni, G., Z. Xu, A. M. Mohamed, H. Li, X. Tang *et al.*, 2013 Experimental evidence for UNC-6 (netrin) axon guidance by stochastic fluctuations of intracellular UNC-40 (DCC) outgrowth activity. Biol Open 2**:** 1300-1312.

Lai Wing Sun, K., J. P. Correia and T. E. Kennedy, 2011 Netrins: versatile extracellular cues with diverse functions. Development 138**:** 2153-2169.

Leung-Hagesteijn, C., A. M. Spence, B. D. Stern, Y. Zhou, M. W. Su *et al.*, 1992 UNC-5, a transmembrane protein with immunoglobulin and thrombospondin type 1 domains, guides cell and pioneer axon migrations in C. elegans. Cell 71**:** 289-299.

Levy-Strumpf, N., and J. G. Culotti, 2014 Netrins and Wnts function redundantly to regulate antero-posterior and dorso-ventral guidance in C. elegans. PLoS Genet 10**:** e1004381.

Li, H., G. Kulkarni and W. G. Wadsworth, 2008 RPM-1, a Caenorhabditis elegans protein that functions in presynaptic differentiation, negatively regulates axon outgrowth by controlling SAX-3/robo and UNC-5/UNC5 activity. J Neurosci 28**:** 3595-3603.

Lim, Y. S., S. Mallapur, G. Kao, X. C. Ren and W. G. Wadsworth, 1999 Netrin UNC-6 and the regulation of branching and extension of motoneuron axons from the ventral nerve cord of Caenorhabditis elegans. J Neurosci 19**:** 7048-7056.

MacNeil, L. T., W. R. Hardy, T. Pawson, J. L. Wrana and J. G. Culotti, 2009 UNC-129 regulates the balance between UNC-40 dependent and independent UNC-5 signaling pathways. Nat Neurosci 12**:** 150-155.

Maes, T., A. Barcelo and C. Buesa, 2002 Neuron navigator: a human gene family with homology to unc-53, a cell guidance gene from Caenorhabditis elegans. Genomics 80**:** 21-30.

Manser, J., C. Roonprapunt and B. Margolis, 1997 C. elegans cell migration gene mig-10 shares similarities with a family of SH2 domain proteins and acts cell nonautonomously in excretory canal development. Dev Biol 184**:** 150-164.

Manser, J., and W. B. Wood, 1990 Mutations affecting embryonic cell migrations in Caenorhabditis elegans. Dev Genet 11**:** 49-64.

McShea, M. A., K. L. Schmidt, M. L. Dubuke, C. E. Baldiga, M. E. Sullender *et al.*, 2013 Abelson interactor-1 (ABI-1) interacts with MRL adaptor protein MIG-10 and is required in guided cell migrations and process outgrowth in C. elegans. Dev Biol 373**:** 1-13.

Meinhardt, H., and A. Gierer, 2000 Pattern formation by local self-activation and lateral inhibition. Bioessays 22**:** 753-760.

Merz, D. C., H. Zheng, M. T. Killeen, A. Krizus and J. G. Culotti, 2001 Multiple signaling mechanisms of the unc-6/netrin receptors unc-5 and unc-40/dcc in vivo. Genetics 158**:** 1071-1080.

Moore, S. W., M. Tessier-Lavigne and T. E. Kennedy, 2007 Netrins and their receptors. Adv Exp Med Biol 621**:** 17-31.

Morikawa, R. K., T. Kanamori, K. Yasunaga and K. Emoto, 2011 Different levels of the Tripartite motif protein, Anomalies in sensory axon patterning (Asap), regulate distinct axonal projections of Drosophila sensory neurons. Proc Natl Acad Sci U S A 108**:** 19389-19394.

Norris, A. D., and E. A. Lundquist, 2011 UNC-6/netrin and its receptors UNC-5 and UNC-40/DCC modulate growth cone protrusion in vivo in C. elegans. Development.

Pan, C. L., J. E. Howell, S. G. Clark, M. Hilliard, S. Cordes *et al.*, 2006 Multiple Wnts and frizzled receptors regulate anteriorly directed cell and growth cone migrations in Caenorhabditis elegans. Dev Cell 10**:** 367-377.

Poinat, P., A. De Arcangelis, S. Sookhareea, X. Zhu, E. M. Hedgecock *et al.*, 2002 A conserved interaction between beta1 integrin/PAT-3 and Nck-interacting kinase/MIG-15 that mediates commissural axon navigation in C. elegans. Curr Biol 12**:** 622-631.

Poon, V. Y., M. P. Klassen and K. Shen, 2008 UNC-6/netrin and its receptor UNC-5 locally exclude presynaptic components from dendrites. Nature.

Quinn, C. C., D. S. Pfeil, E. Chen, E. L. Stovall, M. V. Harden *et al.*, 2006 UNC-6/netrin and SLT-1/slit guidance cues orient axon outgrowth mediated by MIG-10/RIAM/lamellipodin. Curr Biol 16**:** 845-853.

Quinn, C. C., D. S. Pfeil and W. G. Wadsworth, 2008 CED-10/Rac1 mediates axon guidance by regulating the asymmetric distribution of MIG-10/lamellipodin. Curr Biol 18**:** 808-813.

Ren, X. C., S. Kim, E. Fox, E. M. Hedgecock and W. G. Wadsworth, 1999 Role of netrin UNC-6 in patterning the longitudinal nerves of Caenorhabditis elegans. J Neurobiol 39**:** 107-118.

Shakir, M. A., J. S. Gill and E. A. Lundquist, 2006 Interactions of UNC-34 Enabled with Rac GTPases and the NIK kinase MIG-15 in Caenorhabditis elegans axon pathfinding and neuronal migration. Genetics 172**:** 893-913.

Song, S., Q. Ge, J. Wang, H. Chen, S. Tang *et al.*, 2011 TRIM-9 functions in the UNC-6/UNC-40 pathway to regulate ventral guidance. Journal of genetics and genomics = Yi chuan xue bao 38**:** 1-11.

Stringham, E., N. Pujol, J. Vandekerckhove and T. Bogaert, 2002 unc-53 controls longitudinal migration in C. elegans. Development 129**:** 3367-3379.

Stringham, E. G., and K. L. Schmidt, 2009 Navigating the cell: UNC-53 and the navigators, a family of cytoskeletal regulators with multiple roles in cell migration, outgrowth and trafficking. Cell adhesion & migration 3**:** 342-346.

Tang, X., and W. G. Wadsworth, 2014 SAX-3 (Robo) and UNC-40 (DCC) Regulate a Directional Bias for Axon Guidance in Response to Multiple Extracellular Cues. PLoS One 9**:** e110031.

Tessier-Lavigne, M., and C. S. Goodman, 1996 The molecular biology of axon guidance. Science 274**:** 1123-1133.

Teulière, J., C. Gally, G. Garriga, M. Labouesse and E. Georges-Labouesse, 2011 MIG-15 and ERM-1 promote growth cone directional migration in parallel to UNC-116 and WVE-1. Development 138**:** 4475-4485.

Wadsworth, W. G., H. Bhatt and E. M. Hedgecock, 1996 Neuroglia and pioneer neurons express UNC-6 to provide global and local netrin cues for guiding migrations in C. elegans. Neuron 16**:** 35-46.

Wadsworth, W. G., and E. M. Hedgecock, 1996 Hierarchical guidance cues in the developing nervous system of C. elegans. Bioessays 18**:** 355-362.

Wang, Q., and W. G. Wadsworth, 2002 The C domain of netrin UNC-6 silences calcium/calmodulin-dependent protein kinase- and diacylglycerol-dependent axon branching in Caenorhabditis elegans. J Neurosci 22**:** 2274-2282.

Wang, Z., Y. Hou, X. Guo, M. van der Voet, M. Boxem *et al.*, 2013 The EBAX-type Cullin-RING E3 ligase and Hsp90 guard the protein quality of the SAX-3/Robo receptor in developing neurons. Neuron 79**:** 903-916.

Wang, Z., L. M. Linden, K. M. Naegeli, J. W. Ziel, Q. Chi *et al.*, 2014 UNC-6 (netrin) stabilizes oscillatory clustering of the UNC-40 (DCC) receptor to orient polarity. J Cell Biol 206**:** 619-633.

Xu, Y., H. Taru, Y. Jin and C. C. Quinn, 2015 SYD-1C, UNC-40 (DCC) and SAX-3 (Robo) function interdependently to promote axon guidance by regulating the MIG-2 GTPase. PLoS Genet 11**:** e1005185.

Xu, Z., H. Li and W. G. Wadsworth, 2009 The roles of multiple UNC-40 (DCC) receptor-mediated signals in determining neuronal asymmetry induced by the UNC-6 (netrin) ligand. Genetics 183**:** 941-949.

Yang, Y., W. S. Lee, X. Tang and W. G. Wadsworth, 2014 Extracellular Matrix Regulates UNC-6 (Netrin) Axon Guidance by Controlling the Direction of Intracellular UNC-40 (DCC) Outgrowth Activity. PLoS One 9**:** e97258.

Yoshimura, S., J. I. Murray, Y. Lu, R. H. Waterston and S. Shaham, 2008 mls-2 and vab-3 Control glia development, hlh-17/Olig expression and glia-dependent neurite extension in C. elegans. Development 135**:** 2263-2275.

Zallen, J. A., B. A. Yi and C. I. Bargmann, 1998 The conserved immunoglobulin superfamily member SAX-3/Robo directs multiple aspects of axon guidance in C. elegans. Cell 92**:** 217-227.

Ziel, J. W., E. J. Hagedorn, A. Audhya and D. R. Sherwood, 2009 UNC-6 (netrin) orients the invasive membrane of the anchor cell in C. elegans. Nat Cell Biol 11**:** 183-189.

Figure 1. Model for UNC-40 self-organizing polarization and random walk movement. (**A**) Along the plasma membrane, complexes comprising UNC-40 and UNC-5 interact with extracellular cues. A self-organizing process is triggered. In wild-type animals (top) there is a high probability that complexes associated with specific levels of the extracellular cues will mediate outgrowth activity. Compared to wildtype, in animals with loss of UNC-5 function (bottom) the probability of these same complexes mediating outgrowth activity is lower and the probability that the other complexes instead will mediate outgrowth is higher. Direction is labeled left, down, and right, in reference to the orientation of the figure and to emphasize that the model is not referring to any specific cues or their sources in the animal. (**B**) Two sets of tracks are shown to compare random walk models derived from representative wildtype and mutant experimental results. Compared to wildtype, the mutant has a lower probability of outgrowth in one specific direction (down) and a higher probability of outgrowth in other directions (left and right). Using the probability distributions shown below the tracks, 50 simulated random walks of 500 steps were plotted from an origin. This comparison emphasizes that even though the direction of movement is the same, there is a difference in the average displacement. We propose this property of movement is manifested during neuronal extension in wildtype and mutant animals as a difference in the rate of outgrowth. In statistical physics, net movement through the action of random motion is diffusion. Here, each track models the trajectory that mass of the plasma membrane could move during extension. The probability density function of the position of the mass as a function of space and time is described by an advection-diffusion equation. In summary, we suggest that the advection-diffusion model can be used to describe the process by which mass at the leading edge of an extension is transported and that our results describe how genes regulate this transport.

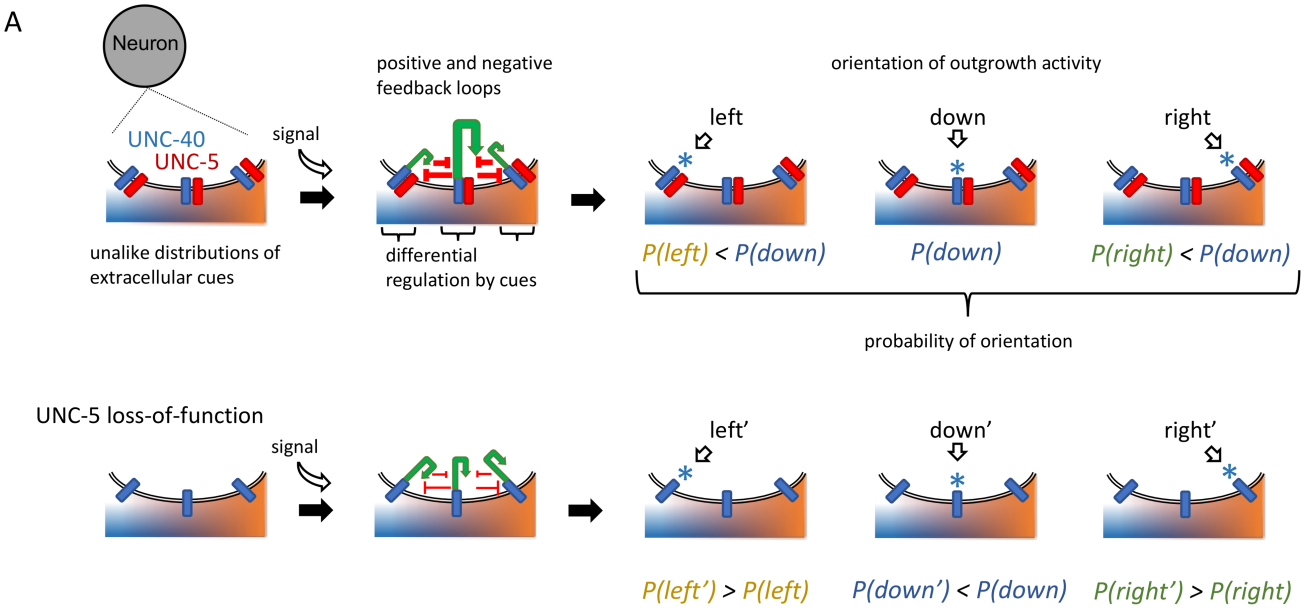

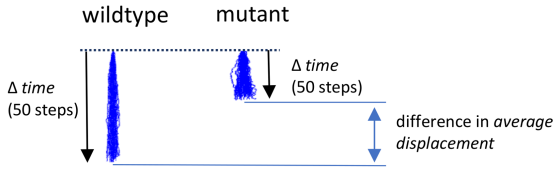

Example:						
	P(right)	=	0.1	0.33	=	*P(right')*
	P(left)	=	0.1	0.33	=	*P(left')*
	P(down)	=	0.8	0.33	=	*P(down')*

Figure 2. Model for outgrowth movement based on the SOAL model. Schematic diagrams of the outgrowth of a neuron (gray) through an environment of multiple extracellular cues. These cues may be molecules presented at the surfaces of surrounding cells and extracellular matrix. The extracellular cues are represented here as color gradients of purple, blue, and orange. Outgrowth activity is mediated at the surface of the neuron through receptor activity. UNC-40-mediated activity is depicted in red, and nonUNC-40-mediated in green. The relative probability of activity along the surface is represented by the extent to which the colored areas cover the neuron's surface. Increasing the degree to which the direction of activity fluctuates over time decreases the extent of outward movement. Random walk models depicting this property are shown above each diagram. See text for details. **(A)** Depicted is the movement of a neuronal extension towards a source of a cue(s) (orange). At time 1 (top) the probability of outgrowth towards the source is high, however at time 2 (bottom) the probability of outgrowth in other directions increases as more receptors away from the leading edge are stimulated due to the higher concentration of the cue. This increases the degree to which the direction of activity fluctuates over time and decreases the extent of outward movement. **(B)** Depicted is the movement of a neuronal extension in wildtype (top) and an *unc-5* mutant (bottom). Loss of UNC-5 affects the UNC-40 SOAL process and causes more receptor activity away from the leading edge, thus decreasing the probability of outgrowth towards the source and increasing the probability of outgrowth in other directions. This increases the degree to which the direction of activity fluctuates over time and decreases the extent of outward movement. Under the same conditions, the rate of outward movement is reduced in *unc-5* mutants as compared to wildtype.

1161

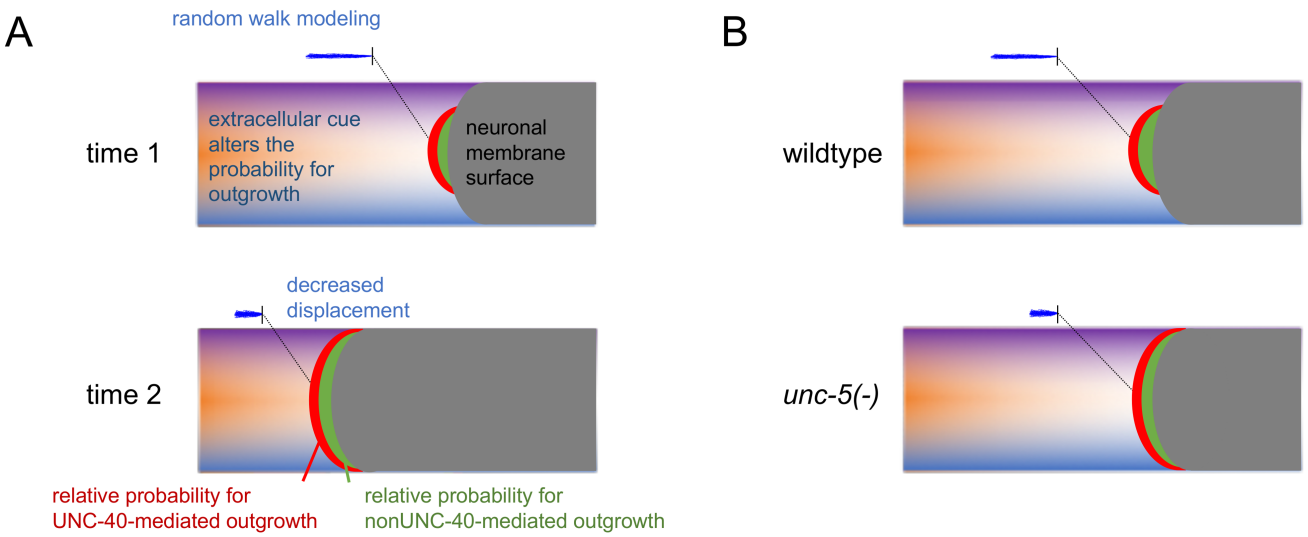

1162

1163

Figure 3. UNC-5 regulates the patterning of outgrowth extensions from HSN. (**A**) Photomicrographs of HSN at the L1, L2, and adult stages in wildtype and *unc-5(e53)* mutants. In L1 and L2 animals neurite extensions (arrows) are often observed in wild-type animals but are more rare in *unc-5* mutants. The short ventral migration of the cell body that occurs in wild-type animal sometimes fails in *unc-5* mutants, leaving the cell body farther from the PLM axon (arrowhead) with a single longer ventral extension. The position of the cell body remains dorsal. Scale bar: 10 μm. (**B**) The percentage of HSN neuron with 0, 1, or more than 1 neurite extension at the L1 stage. In *unc-5* mutants nearly half of the neurons do not extend a process. Error bars indicated the standard error mean; n values are indicated above each column. Significant differences (two-tailed t-test), *P<0.001. (**C**) The percentage of HSN neurons with a single long extension at the L2 stage. Several *unc-5* alleles were tested as described in the text. In mutants with loss-of-function there is more often a single extension from the cell body and the cell body is dorsally mispositioned. (**D**) Photomicrographs of HSN at the early L4, late L4, and adult stages in wildtype and in animals expressing UNC-6ΔC. The expression of UNC-6ΔC induces multiple processes, most often two major extensions, that are guided ventrally. (**E**) The percentage of HSN neurons with a cell body mispositioned dorsally at the L2 stage. In loss-of-function mutants the cell body often fails to undertake a short ventral migration during the L2 stage. The migration is not delayed, but rather it remains dorsal. (**F**) The percentage of HSN neurons with multiple ventral extensions at the L4 stage. The additional processes induced by UNC-6ΔC can be suppressed by *unc-5* and *mig-10* mutations. Additional processes induced by *mig-15(rh148)* can also be suppressed by the *unc-5* mutation. (**G**) Photomicrographs of HSN at adult stages in a *mig-15* mutant. Similar to UNC-6ΔC expression, *mig-15* mutations can also cause additional processes that are guided ventrally (YANG *et al.* 2014).

1189

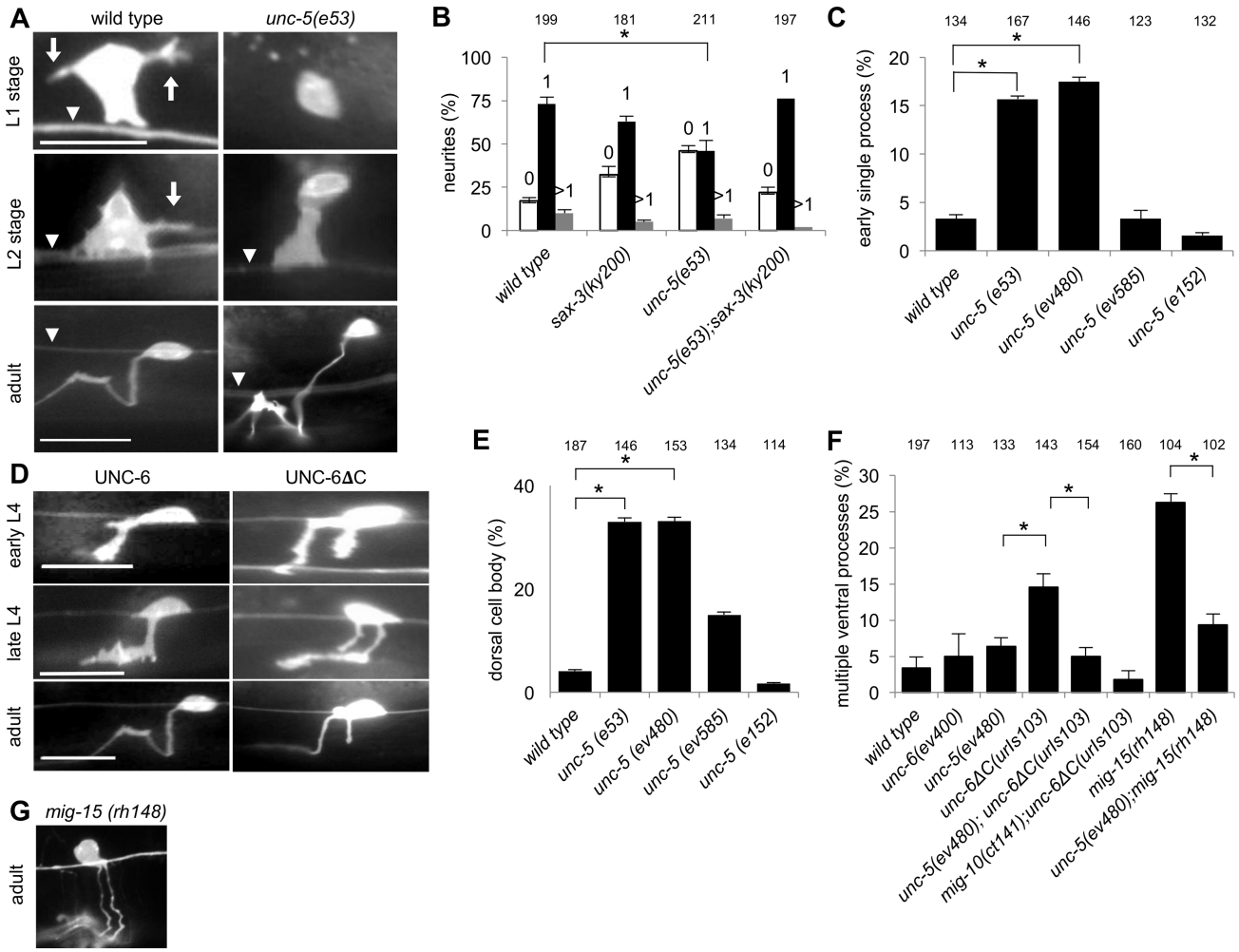

1190

Figure 4 UNC-5 regulates the patterning of extension from ALM, AVM, and PLM. (**A**) Photomicrographs of the ALM, AVM, and PLM neurons at the L4 stage in wild-type animals and *mig-15* mutants. In wildtype (top) a single PLM axon travels anteriorly from the posterior cell body (not shown). Near the vulva (arrow) the axon branches; one branch extends to the ventral nerve chord and another extends anteriorly. The anterior extension terminates before reaching the area of the ALM cell body. In *mig-15* mutants the PLM can extend anteriorly past the ALM cell body (bottom). (**B**) The percentage of PLM neurons where the PLM neuron extend anteriorly past the ALM cell body. The anterior extension often over-extends in *mig-15* mutants. Loss of *unc-5* or *unc-40* function can suppress this phenotype. (**C**) Photomicrographs of the ALM and AVM neurons at the L4 stage in wild-type animals and mutants showing different patterns of outgrowth extension. In wildtype (top) a single axon travels anteriorly to the nerve ring (arrowheads). At the nerve ring the axon branches; one branch extends further anteriorly and the other extends into the nerve ring. In mutants, one or both axons may only extend anteriorly and will not extend into the nerve ring (second from top). Or one or both axons will only extend into the nerve ring and will not extend anteriorly (third from top). Or one or both axons will fail to extend into either the nerve ring or anteriorly (bottom). Scale bar: 20 µm. (**D**) The percentage of AVM neurons where the AVM neuron failed to extend into the nerve ring. The neuron often fails to extend in the *unc-40* and *mig-15;unc-5* mutants, whereas it does extend in the *mig-15, unc-5,* and *mig-15;unc-40* mutants. Error bars indicated the standard error mean; n values are indicated above each column. Significant differences (two-tailed t-test), *P<0.001. (**E**) The percentage of AVM neurons where the AVM neuron failed to extend anteriorly, past the nerve ring. The neuron often fails to extend anteriorly in the *mig-15;unc-5* mutants, whereas it does extend in the *mig-15, unc-5, unc-40,* and *unc-40;mig-15* mutants. There is a significant difference between the *unc-40* and *unc-40;mig-15* mutants.

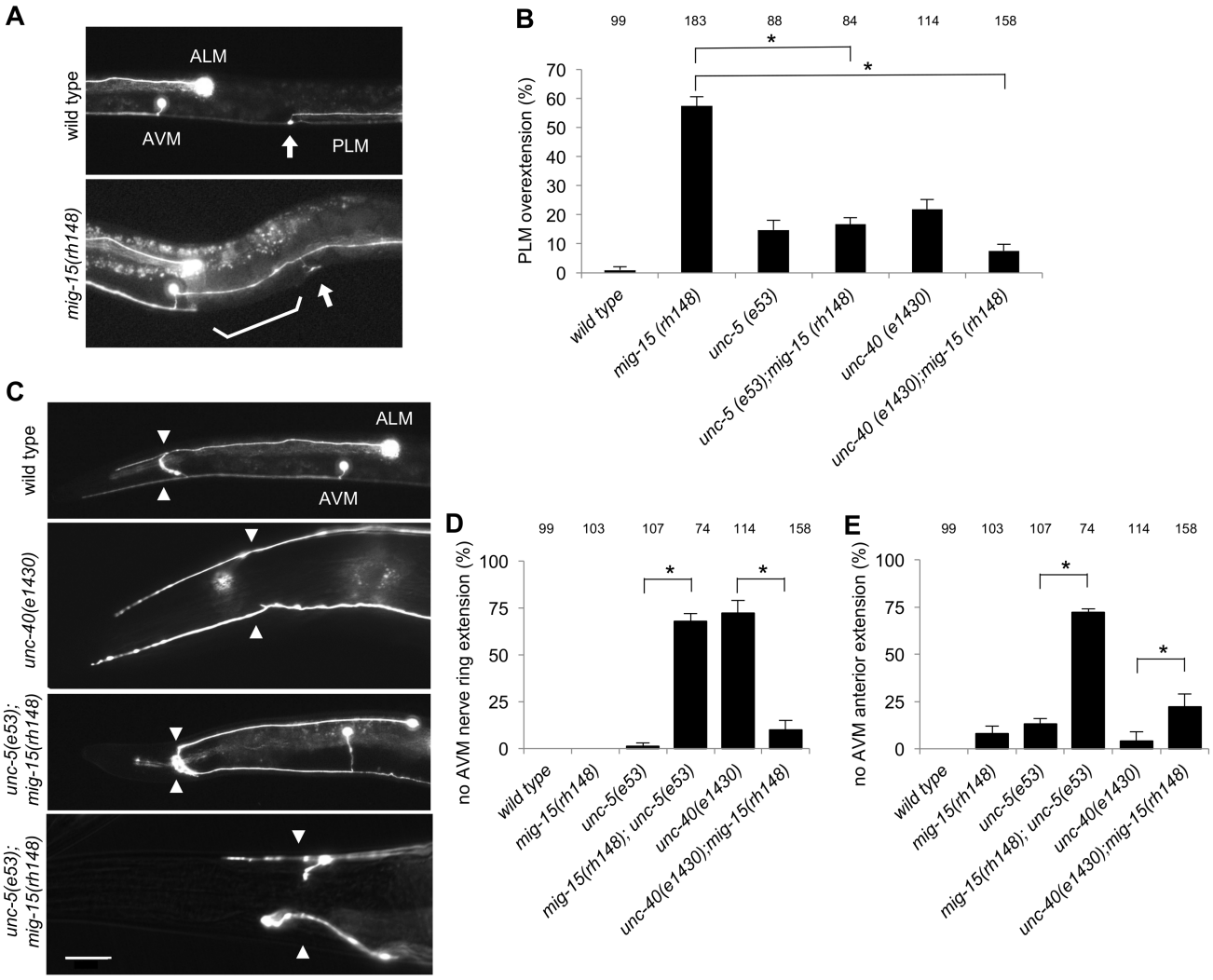

Figure 5 Assay to measure the effects a mutation has on movement. (**A**) The direction of outgrowth extension from the HSN cell body can vary and whether the axon developed in the dorsal, anterior, posterior, or ventral direction in L4 stage animals is scored (left panel). This creates a probability distribution in which the direction (*X*) is a random variable (center panel). A simple random walk is generated by using the same probability distribution for a succession of steps with an equal time interval (right panel). (**B**) For wildtype and two mutants, 50 simulated random walks of 500 steps were plotted from an origin (0,0). The results graphically indicate the directional bias for movement. For random walk movement created in mutant A (red, results from *unc-5(e53)*), the directional bias is shifted anteriorly (left) relative to wildtype. The results also graphically show the displacement of movement. For random walk movement created in mutant B (blue, results from *egl-20(n585);sax-3(ky123)*), the average of the final position (displacement) from the origin is a much shorter distance than wildtype. (**C**) Plots of the normal distribution of the final position along the x axis of the random walk tracks shown in B. The mean position for each is set at 0. The plots graphically illustrate how random walks constructed from the probability distribution for the direction of outgrowth extensions can reveal a diffusion process.

1236

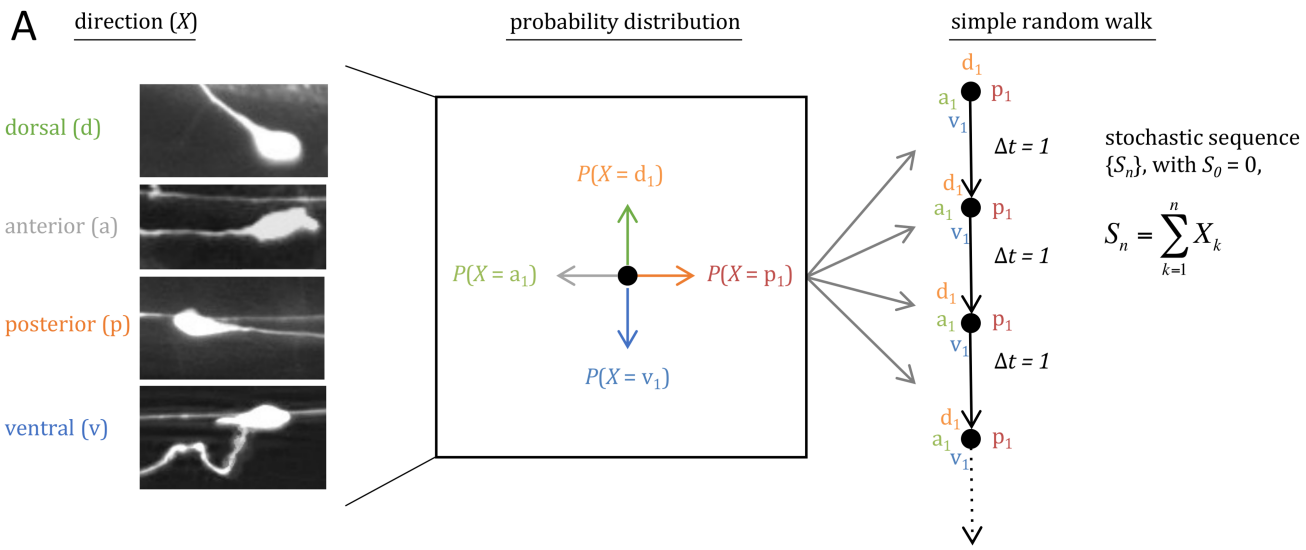

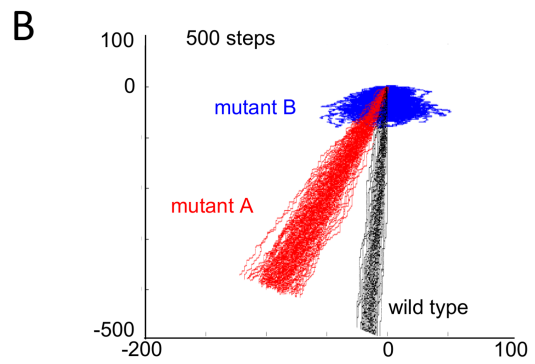

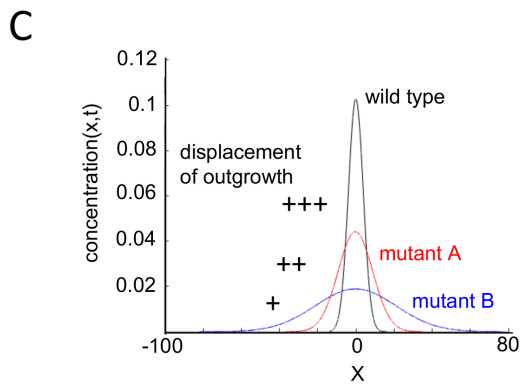

1237

Figure 6. Mutations have different effects on movement. Examples of random walk analyses using the direction of axon development from the HSN neuron in different mutants (Table 1). The graphs were created as described in the figure legend of Figure 3. For each panel, plots are shown for the normal distribution of the final position along the x axis for the random walk tracks plotted in the inserts. The inserts depict the random walk movement that would be produced by the probability distribution for the direction of outgrowth in the mutant. Plots derived from the same data are colored alike. Each panel depicts the analyses of four different mutants and wildtype. Three different distribution patterns are observed: (1) the wild-type distribution, which has the distribution curve with the highest peak; (2) the *unc-5, egl-20, unc-53,* and *unc-6* (not shown) distribution, which is flatter than the wild-type curve; (3) the *madd-2, sax-3, mig-15,* and double combinations, which have the flattest distribution curve.

1250

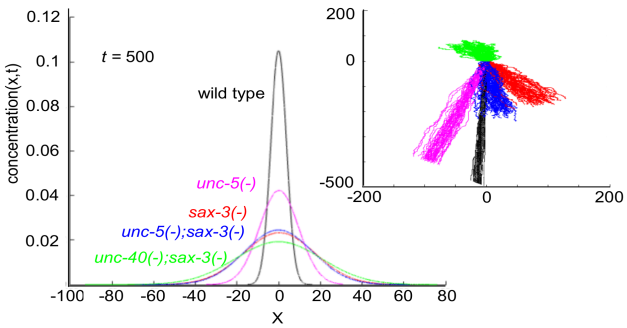

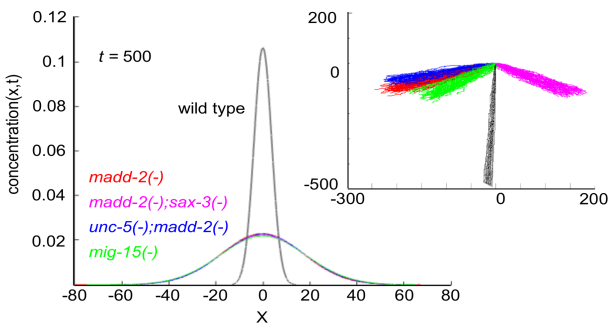

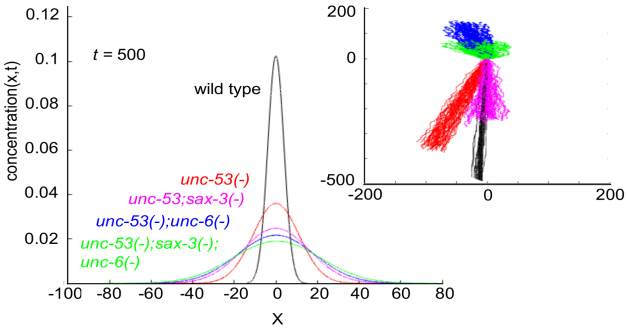

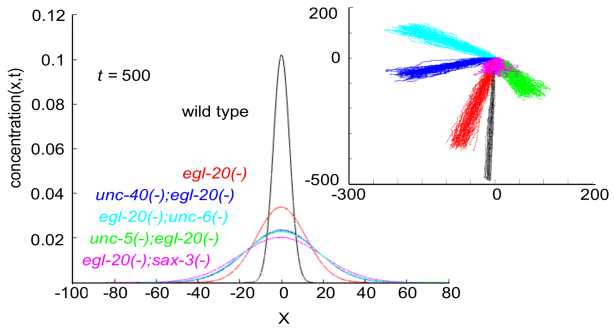

1251

Figure 7. Mutations alter the spatial extent of movement. (**A**) Plotted are the mean squared displacement (MSD) curves as a function of time interval (d*t*). The values are in arbitrary units, since the time scale was arbitrarily set at 1. The curves show the extent that different mutations can alter the MSD relative to wildtype and the MSD caused by an unbiased random walk. For each time interval, mean and s.e.m. are plotted. (**B**) From the slope of MSD curves a coefficient can be derived that gives the relative rate of diffusion. Colored bars correspond to the like-colored curves given in panel A. The coefficients for *unc-5, egl-20, unc-53,* and *unc-6* form a class that is distinct from that derived from wildtype and from the double mutants.

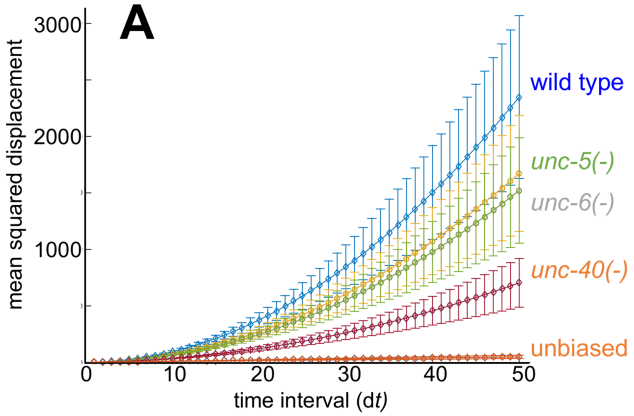

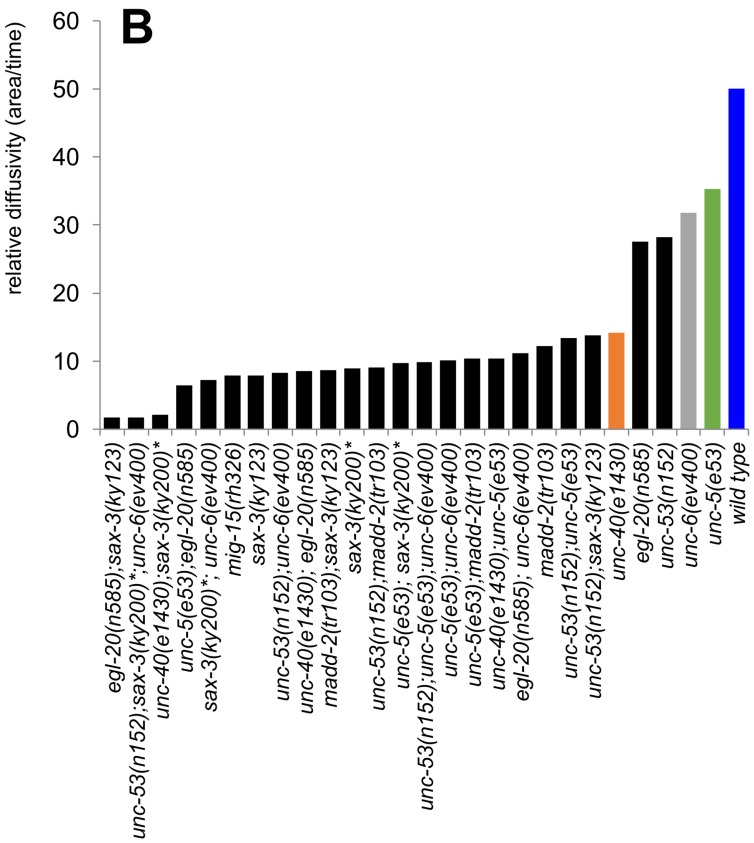

1263
1264

Figure 8. Models for the relationship between UNC-40-mediated outgrowth activity and UNC-40 receptor clustering. (A) In this model the self-organizing UNC-40 SOAL process causes observable UNC-40 receptor clustering. Receptor clusters become stable and exit the SOAL process, at which point they recruit the outgrowth machinery. Whereas the direction of asymmetric receptor localization is determined stochastically, the direction of outgrowth is determined by the site of stabilization. **(B)** In this model the self-organizing UNC-40 SOAL process is coupled to the outgrowth machinery. The direction of both asymmetric receptor localization and outgrowth activity are stochastically determined. Observable receptor clustering may arise over time and these sites may become paramount for outgrowth movement, but cluster formation is not a prerequisite for outgrowth activity. Conceptually, in both models the site of outgrowth activity is determined by where UNC-40 receptor complexes recruit the outgrowth machinery, however the second model postulates situations where there are innumerable fluctuating sites that create outgrowth movement in various directions. Because the effect at each instance of time of every outgrowth event is immeasurable, outgrowth in this model is considered as a continuous stochastic process that evolves over time.

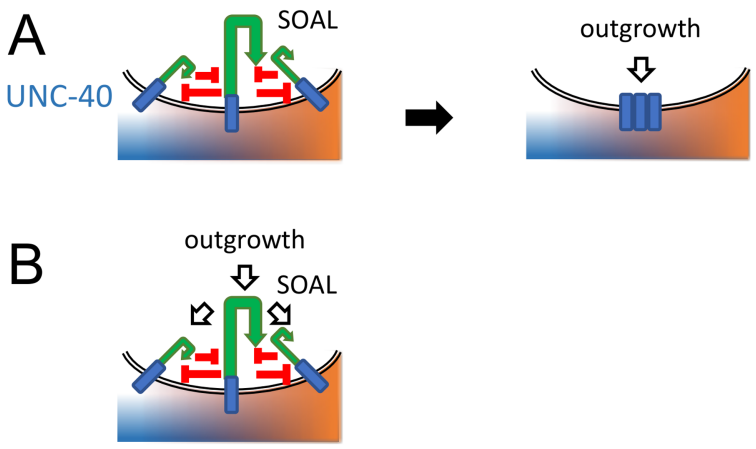

1286

1287

Figure 9. Mutations affect asymmetric intracellular UNC-40::GFP localization. (**A**) Graph indicating the dorsal-ventral localization of UNC-40::GFP in HSN. The graph shows the average ratio of dorsal-to-ventral intensity from linescan intensity plots of the UNC-40::GFP signal around the periphery of the HSN cell. UNC-40::GFP is ventrally localized in wildtype, but the ratio is different in the mutants. Error bars represent standard error of mean. Below is a graphic representation of the possible UNC-40 localization patterns when the intensity ratio is ≥ 1 or is <1. (**B**) Graph indicating the anterior-posterior localization of UNC-40::GFP. To determine orientation, line-scan intensity plots of the UNC-40::GFP signal across the dorsal periphery of the HSN cell were taken, the dorsal surface was geometrically divided into three equal segments, and the total intensity of each was recorded. The percent intensity was calculated for each segment and ANOVA was used to determine if there is a significant difference between the three segments (see Material and Methods). Whereas in the *unc-5* and *egl-20* mutants there is a bias for anterior or posterior localization, there is a uniform distribution in *unc-5;egl-20* double mutants. Uniform distribution is also observed in strong loss-of-function *sax-3* and *madd-2* mutants. (*) Animals grown at the *sax-3(ky200)* restrictive temperature (25°C). Below is a graphic representation of the possible UNC-40 localization patterns.

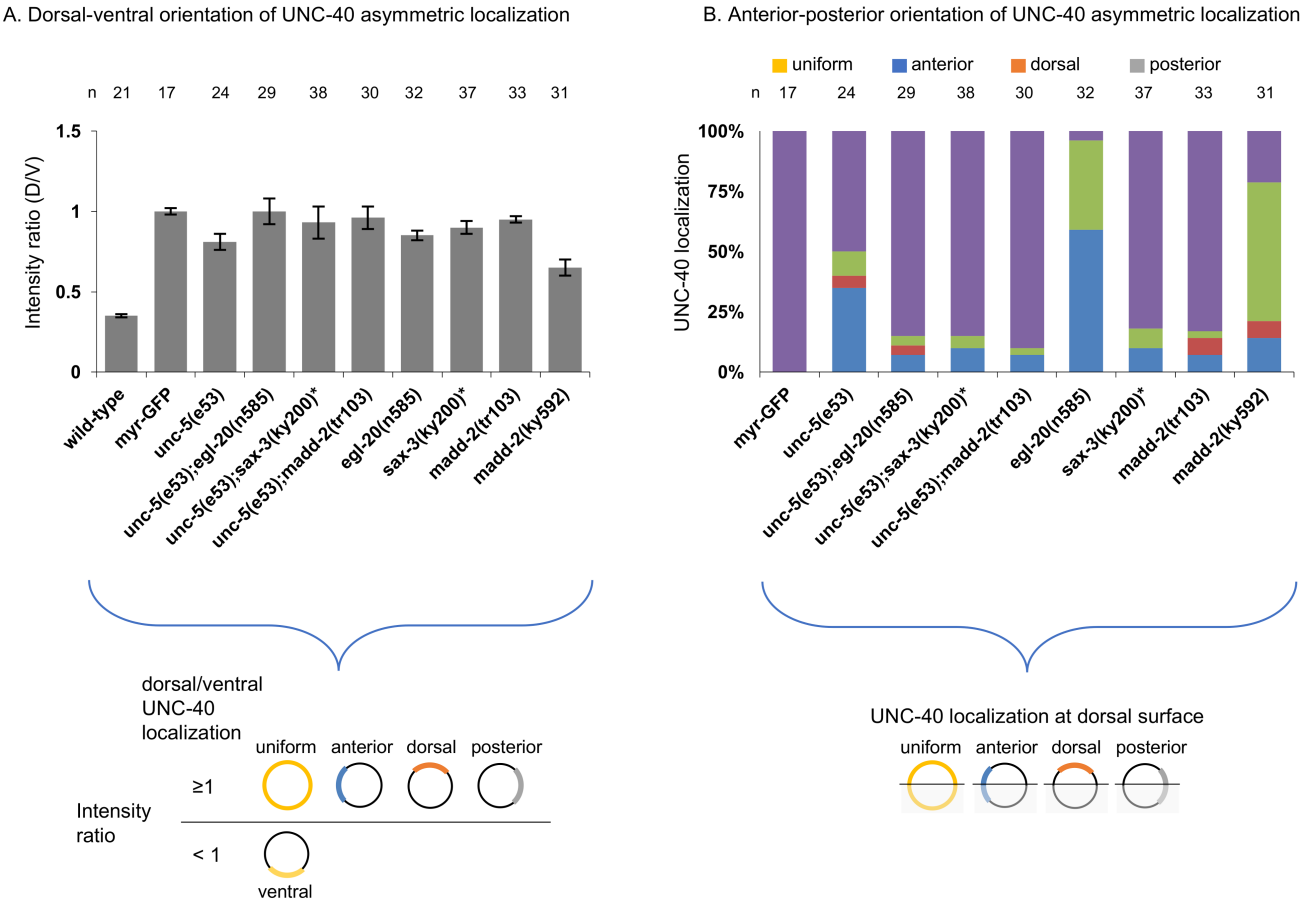

1306

1307

Figure 10. Model for the outgrowth movement of PLM. Schematic diagrams of the anteriorly directed outgrowth of PLM. The elements of the schematics are described in Figure 2. **(A)** At each of the four positions an extension encounters different levels of extracellular cues. At position 3, a cue(s) is present that inhibits outgrowth activity. PLM extension terminates in this area in wildtype, but in some mutants there is an overextension to position 4. **(B)** Depicted are the effects that extracellular cues have on the relative probabilities of UNC-40-mediated and nonUNC-40-mediated outgrowth activity at the different positions. At position 3 in wildtype the degree to which the direction of outgrowth activity fluctuates increases and the extent of outgrowth movement decreases, stalling outgrowth. Because the SOAL process is perturbed in the mutants, at position 3 the probability of outgrowth activity perpendicular to the direction bias does not increase as much as in wildtype and the probability of anterior outgrowth activity remains greater. This allows a stronger directional bias to persist, allowing forward extension. To illustrate the concept, random walk models are shown which were constructed using the indicated values for outgrowth in the anterior, dorsal, and ventral directions. See text for details.

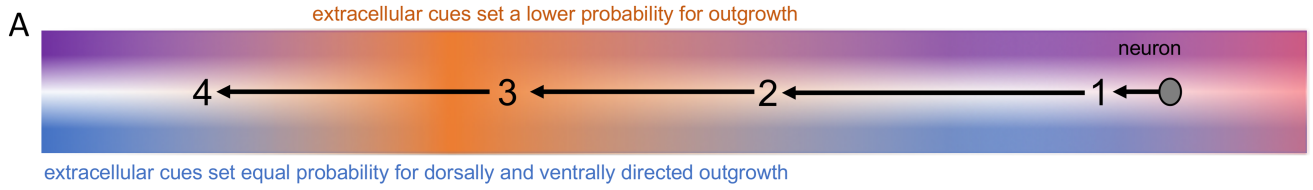

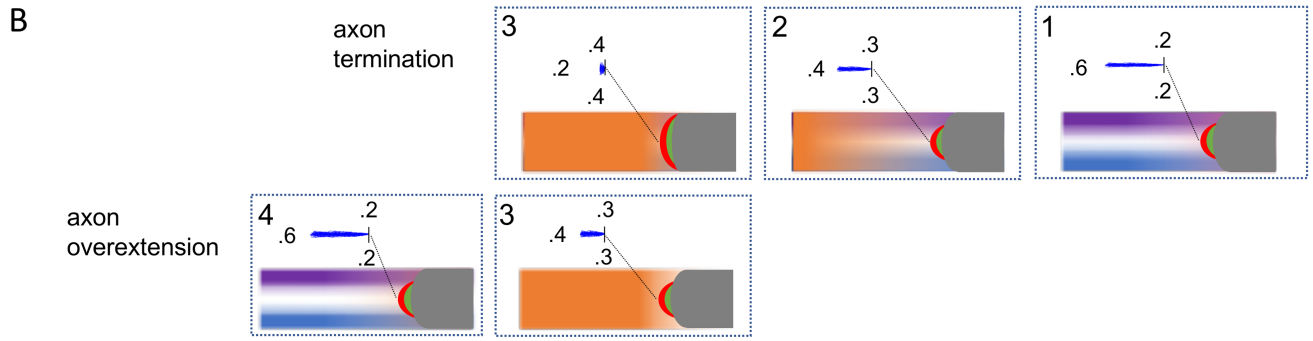

1325

1326

Figure 11. Model for the effects that mutations have on the outgrowth movement of PLM. Schematic diagrams of PLM outgrowth at position 3 of Figure 10 in wildtype and mutants. The elements of the schematics are described in Figure 2. PLM outgrowth terminates in wildtype, *unc-40*, and *unc-5;mig-15* mutants, but overextends in *mig-15* mutants. See text for details.

figure 10, position 3

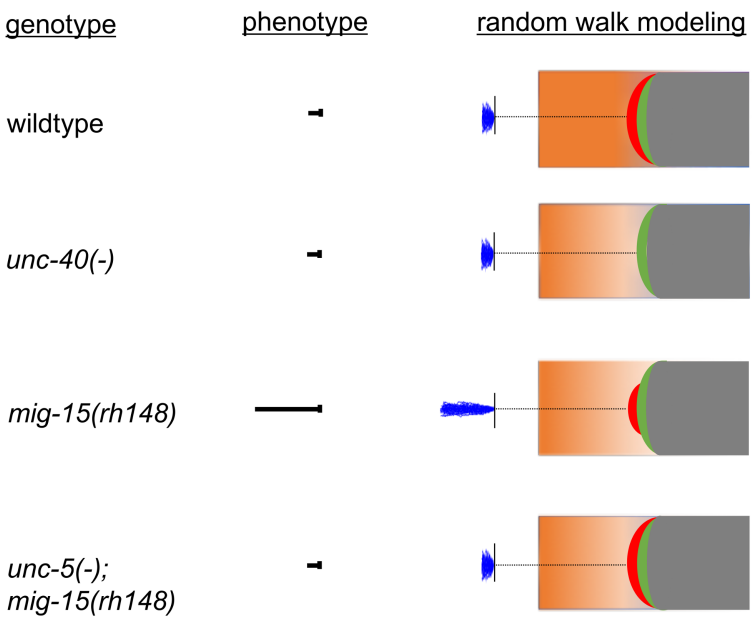

Figure 12. Model for the outgrowth movement of AVM at the nerve ring. Schematic diagrams of the outgrowth of AVM at the nerve ring. The elements of the schematics are described in Figure 2. **(A)** At each of the four positions an extension encounters different levels of extracellular cues. At position 2, a cue(s) at the nerve ring promotes UNC-40-mediated outgrowth activity. From this position in wildtype, AVM extends further anteriorly and also dorsally along the nerve ring. However, in some mutants either the anterior or dorsal extension is absent. In other mutants, extension in both directions is absent. **(B)** Depicted are the effects that extracellular cues have on the relative probabilities of UNC-40-mediated and nonUNC-40-mediated outgrowth activity at the different positions. At position 2 in wildtype the extracellular cues create a weak bias for outgrowth in both the anterior and dorsal directions. Further dorsally at position 3, cues create an equal probability for outgrowth in the anterior and posterior directions, allowing the nerve ring cue that promotes UNC-40-mediated outgrowth to maintain a dorsal directional bias. Further anteriorly at position 4, cues create an equal probability for outgrowth in the dorsal and ventral directions, allowing anterior cues that promote outgrowth to create an anterior directional bias. To illustrate the concept, random walk models are shown which were constructed using the indicated values for outgrowth in the indicated directions. See text for details.

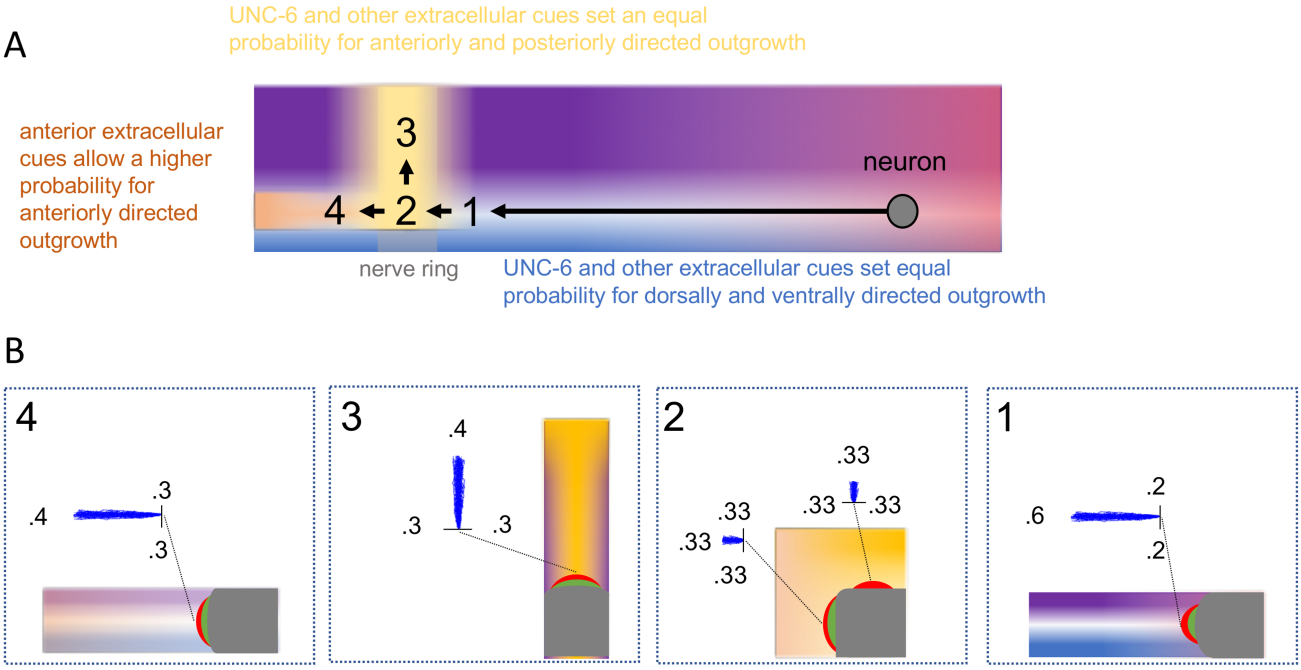

1357

1358

Figure 13. Model for the effects that mutations have on the outgrowth movement of AVM at the nerve ring. Schematic diagrams of AVM outgrowth at position 2 of Figure 12 in wildtype and mutants. The elements of the schematics are described in Figure 2. AVM outgrowth extends both anteriorly and dorsally from this position in wildtype, *mig-15,* and *unc-40;mig-15* mutants. Dorsal extensions are often absent in *unc-40* mutants, whereas both anterior and dorsal extensions are absent in *unc-5;mig-15* mutants. See text for details.

figure 12, position 2

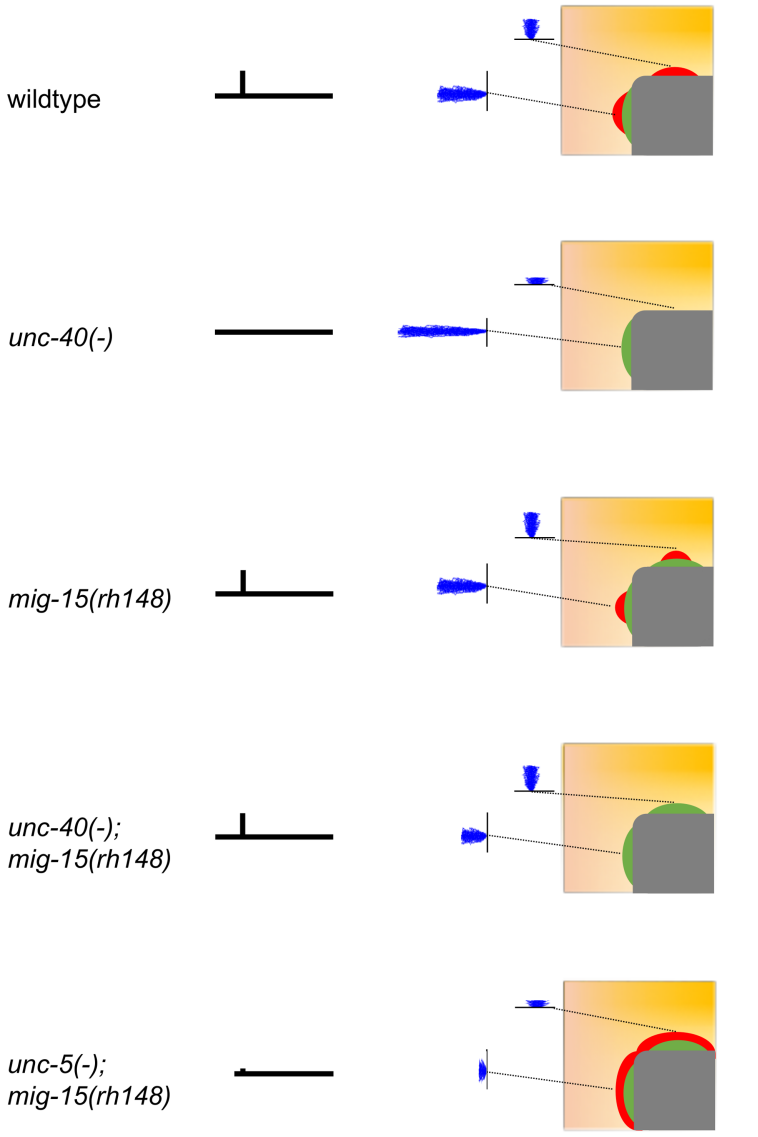

Figure 14. Model for the outgrowth movement of HSN. Schematic diagrams of the ventrally directed outgrowth of HSN. The elements of the schematics are described in Figure 2. **(A)** At each of the three positions an extension encounters different levels of extracellular cues. At position 3, a cue(s) is present that promotes outgrowth activity. At the time when extension is first observed in wildtype, extension is absent in some mutants. Nevertheless, ventral extension will be complete in the mutants at about the same time as in wildtype. **(B)** Depicted are the effects that extracellular cues have on the relative probabilities of UNC-40-mediated and nonUNC-40-mediated outgrowth activity at the different positions. Compared to wildtype, at position 1 in mutants with delayed protrusion the degree to which the direction of outgrowth activity fluctuates is greater and the extent of outgrowth movement is less, resulting in a reduced rate of outgrowth. A weak ventral directional bias develops in the mutant that allows initial ventral extension and by position 2 this ventral bias is stronger. At position 3 in both wildtype and mutant, the degree to which the direction of outgrowth activity fluctuates increases and the extent of outgrowth movement decreases. To illustrate the concept, random walk models are shown which were constructed using the indicated values for outgrowth in the anterior, posterior, and ventral directions. See text for details.

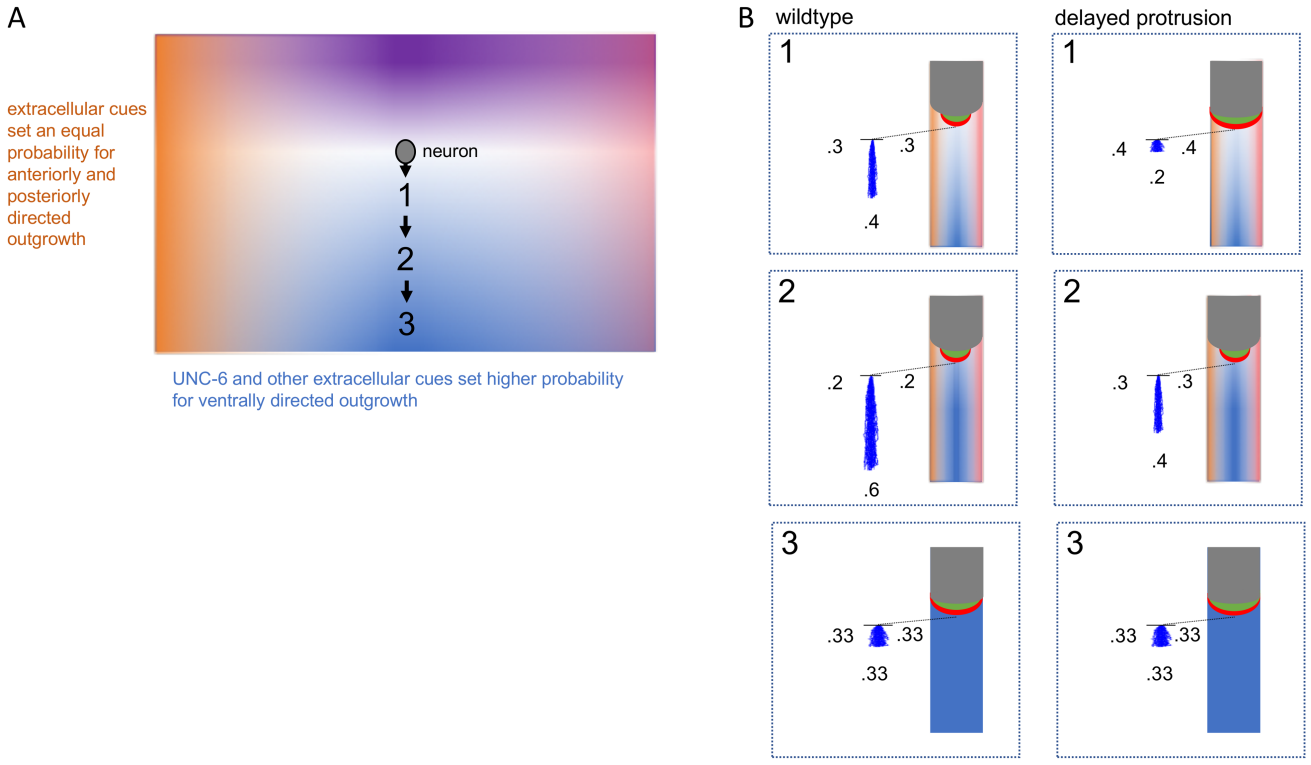

1392

Figure 15. Model for the effects that mutations have on the outgrowth movement of HSN. **(A)** Schematic diagrams of HSN outgrowth at position 1 of Figure 14 in wildtype and mutants. The elements of the schematics are described in Figure 2. HSN outgrowth is delayed in *unc-5* mutants and can develop multiple processes in *mig-15* mutants. The multiple process phenotype is suppressed in *unc-5;mig-15* mutants. See text for details. **(B)** Schematic diagrams of the development of multiple process that maintain the same directional bias. The process is shown in three steps. At the first step, UNC-40 receptors (blue rectangles) are trafficked to the membrane as part of the UNC-40 SOAL process (blue arrows). At the second step, UNC-5 signaling alters the trafficking, increasing the rates anterior (orange arrows) and posterior (red arrows). By the third step, the rate of outgrowth at the flanking regions is greater. We propose that UNC-40, UNC-5, and UNC-6 can be considered as components of an activator-inhibitor system which allows outgrowth patterns to self-organize. See text for details.

1410

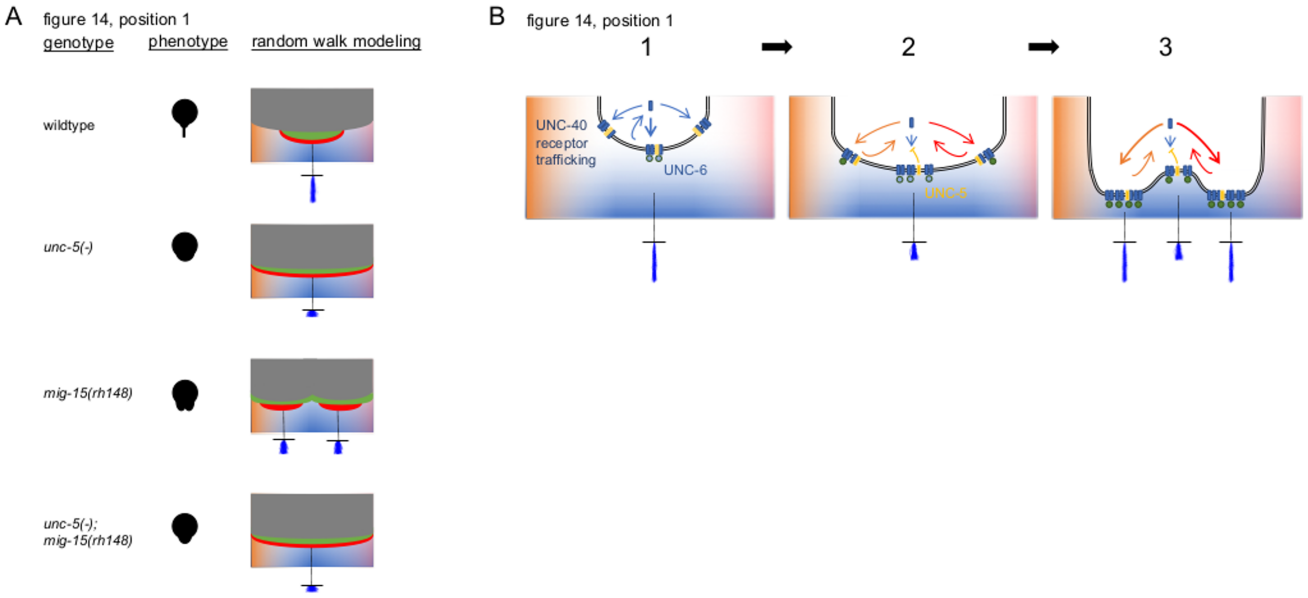

1411

1412

Figure 16. Genetic pathways for self-organizing UNC-40 asymmetric localization. (**A**) Table summarizing the results of experiments previously reported and described in Figure 9 of this paper. (**B**) The genetic data support a model whereby the UNC-6 and EGL-20 extracellular cues regulate at least three pathways leading to robust asymmetric UNC-40 localization. Robust asymmetric UNC-40 localization refers to the ability to observe UNC-40::GFP clustering at the surface of the neuron. Arrows represent activation; bars represent repression. See text for the logic used to construct the pathways.

A

loss-of-function			robust asymmetric UNC-40 localization	reference
unc-6			no	(Kulkarni et al., 2013)
unc-5			yes	(Kulkarni et al., 2013)
unc-5	*unc-6*		no	(Kulkarni et al., 2013)
unc-5	*egl-20*		no	
unc-5	*sax-3*		no	
unc-5	*unc-53*		no	(Kulkarni et al., 2013)
unc-5	*unc-53*	*unc-6*	yes	(Kulkarni et al., 2013)
unc-5	*unc-53*	*sax-3*	no	
unc-5	*madd-2*		no	
unc-6	*unc-53*		yes	(Kulkarni et al., 2013)
unc-6	*sax-3*		no	(Tang and Wadsworth, 2014)
unc-6	*unc-53*	*sax-3*	no	(Tang and Wadsworth, 2014)
egl-20			yes	(Kulkarni et al., 2013)
egl-20	*unc-53*		yes	(Kulkarni et al., 2013)
egl-20	*unc-6*		no	(Kulkarni et al., 2013)
egl-20	*sax-3*		no	(Tang and Wadsworth, 2014)
sax-3			no	(Tang and Wadsworth, 2014)
sax-3	*unc-53*		no	(Tang and Wadsworth, 2014)
unc-53			yes	(Kulkarni et al., 2013)
madd-2			no	
mig-15			yes	(Yang et al., 2014)

B

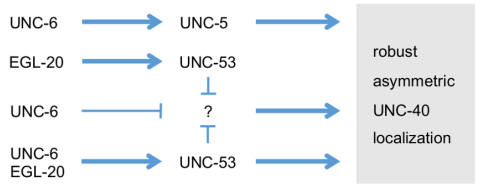

1421